ACTIVE BROWNIAN PARTICLES PROPELLED BY SOUND

by

Serhat Kaya

B.S., Physics, Boğaziçi University, 2014

Submitted to the Institute for Graduate Studies in
Science and Engineering in partial fulfillment of
the requirements for the degree of
Master of Science

Graduate Program in Physics

Boğaziçi University

2016

ACKNOWLEDGEMENTS

I would like to elatedly express my respect and gratitude to my supervisor Assoc. Prof. Mehmet Burçin Ünlü for his endless support and priceless guidance in both my academic career and personal life.

I am also pleasure to Assist. Prof. Giovanni Volpe and his team members Dr. Agnese Callegari, Dr. Masoumeh Mousavi, and Dr. Alessandro Magazzu for their instructive supports.

ABSTRACT

ACTIVE BROWNIAN PARTICLES PROPELLED BY SOUND

Small particles in acoustic fields experience the so-called *acoustic radiation forces* by which the motion of particles can be manipulated in a contact-less way. Active Brownian particles have the ability to propel themselves by converting ambient energy into kinetic energy. However, because of the lack of study, the behavior of active Brownian particles in vicinity of external fields is not well-understood. The usage of acoustic fields in controlling the motion of these particles was suggested before, but this effect has not been resolved analytically yet. In the analysis contained herein, the behavior of active particles inside an acoustic field is investigated by constructing the equation of motion for a single particle. This is the first time in the literature whereby the analytic form of the acoustic radiation forces is integrated with the dynamic equations of the system. The resulting equation is solved via numerical techniques. Then, with the performed simulations for two different active matter models, the collective behavior of active Brownian particles is also exploited.

ÖZET

SESLE İTTİRİLEN AKTİF BROWN PARÇACIKLARI

Akustik alanların içerisindeki küçük parçacıklar *akustik radyasyon kuvveti* olarak adlandırılan bir kuvvete maruz kalırlar ve bu kuvvet parçacıkların hareketlerinin uzaktan kontrol edilmesine olanak sağlar. Aktif Brown parçacıkları ise içinde bulundukları ortamın enerjisini kinetik enerjiye dönüştürerek hareket etme becerisine sahiptirler. Fakat bu parçacıkların harici etki varlığındaki davranışları, çalışma azlığı nedeniyle yeterince anlaşılamıştır. Aktif Brown parçacıklarının hareketlerini kontrol etmek için akustik alanların kullanımı daha önce gündeme gelmiş olmasına karşın, henüz bu etkinin analitik çözümüne dair bir çalışma yoktur. Bu çalışmanın amacı, tek bir parçacığın hareket denklemini kurgulayarak aktif parçacıkların akustik alan içerisindeki davranışlarını incelemektir. Literatürde akustik radyasyon kuvvetinin analitik denklemini aktif parçacıkların dinamik denklemlerine ekleyen ilk çalışma budur. Bulunan denklemlerin nümerik çözümleri kullanılarak iki farklı aktif madde modeli için simulasyonlar yapılmış ve aktif Brown parçacıklarının kolektif davranışları da incelenmiştir.

TABLE OF CONTENTS

LIST OF FIGURES

LIST OF TABLES

LIST OF SYMBOLS

a	A generic known function
b	A generic known function
C	Concentration
D	Diffusion coefficient
D_T	Translational diffusion coefficient
D_R	Rotational diffusion coefficient
Δf	Finite difference of a function
f_1	Monopole scattering coefficient
f_2	Dipole scattering coefficient
F_{ext}	External force
F_{rad}	Acoustic radiation force
F_{trap}	Optical trap force
F_D	Stokes' drag force
g	Strength of the correlation function
k_B	Boltzmann's constant
L	Dimension of the box
m	Mass
N	Number of particles
p_1	First order pressure
p_{in}	Pressure of incoming wave
P_{trap}	Position of the center of the optical trap
Δr	Displacement
R	Radius of the particle
t	time
T	Temperature
v	Velocity
v_1	First order velocity
v_{in}	Velocity of incoming wave

U	External potential
w	Gaussian random numbers
W	Work done on the system
$W(t)$	White noise
Δx	Displacement in x axis
x	Position in x dimension
x_0	Initial position in x dimension
Δy	Displacement in y axis
Δz	Displacement in z axis
γ	Viscous drag coefficient
$\delta(t)$	Dirac-delta function
$\Delta\theta$	Random fluctuation of the direction in Vicsek model
η	Kinematic viscosity of the fluid
θ	Direction angle of velocity in Vicsek model
κ_0	Compressibility of the fluid
κ_p	Compressibility of the particle
κ_{trap}	Stiffness of the optical trap
$\tilde{\kappa}$	Compressibility ratio
λ	Noise of the motion
μ	Acoustic boundary layer
ξ	Gaussian random numbers
$\xi(t)$	Fluctuating force
ρ	Density
$\tilde{\rho}$	Density ratio
τ	Momentum relaxation time
ϕ	Direction angle of the velocity of active Brownian particles
$\phi_i n$	Velocity potential of the incoming wave
ω	Angular frequency of the acoustic waves

LIST OF ACRONYMS/ABBREVIATIONS

1D	One Dimension
2D	Two Dimensions
3D	Three Dimensions
ABP	Active Brownian Particle
ARF	Acoustic Radiation Force

1. INTRODUCTION

The difference between the living entities and inanimate ones constituted one of the hardest questions of human civilization for millenniums. At first implication, one can simply deduce that the movement mechanisms of these two kinds are different than each other. Lifeless bodies move only in presence of external forces such as gravity. On the other hand, vivacious bodies are capable of self-propulsion and can convert their internal energy into mechanical energy. However, with the latest technological developments it became possible to produce artificial machines which have self-propulsion mechanism and translate themselves by using the ambient energy [1]. Even though this talent is one of the basic aspects of life, the term *active* refers to all matter (living or artificial) which have capability to move actively.

Besides self-propulsion mechanisms the collective behavior of active matter is unique. In animal crowds such as flock of birds, schools of fish, or herds of cattle, the communal motion is usually organized because the motion of each individual is affected by the cumulative motion of the whole community [2]. Although there are some basic differences with the motion itself, this collective behavior has similar properties for all the different species of living entities. Moreover, even bacterial colonies in the microscopic scale shows similar attitude. Thermodynamic laws require the system to reach the equilibrium condition as time passes, but because of the energy consumption, active matter systems are capable of drive themselves far from equilibrium [3]. Examples of such systems are macroscopic animals [4, 5], motile cells [6–8], Brownian motors [9], active Brownian particles [10], and artificial self-propelled particles [11, 12].

The first study of modelling of active matter is probably the analysis of Keller and Segel (1970) in which they suggested a mathematical background for chemotactic interaction of amoebae and aggregation [13]. After this work the first computer simulation model for animal groups, called as "boids" model which resembled bird-oid objects was carried out by Reynolds in 1987 [14]. Even though there were many studies on computer simulation of active matter, Vicsek *et al.* (1995) provided a simple but

strong model for self-ordered motion of system of particles [15]. In this model, individual particles had a constant speed and a direction which was the average direction of particles within a circle with a specificed radius centred at the particle, yet it did not explain the behavior of the particles in presence of energy sources. The study which considered the active particles with ability to take up energy from the environment for both continuous and localised energy sources was called *energy depot model* came by Schweitzer *et al.* [16]. This model was generalized by Ebeling *et al.* in 1999 to active Brownian particles with internal energy storage mechanism [10]. Hydrodynamic interactions were added to the energy depot model by Erdmann and Ebeling (2003) [17].

Since there are various types of organisms, their motion shows clear deviations from each other and they are studied separately. For motion of *daphnia*, a microscopic animal, Komin *et al.* (2004) suggested a model which was based on a random motion with a Gaussian angle distribution in the absence of external interactions. A different type of motion, ameboid motion, was analysed by Bödeker *et al.* (2010) by using a Langevin-type stochastic differential equation [6]. A theoretical analysis of sperm movement towards egg which acts as a chemoattractants was carried out by Friedrich and Jülicher in 2007 [7]. Movement of insects was investigated by Kareiva and Shigesada (1983) as a correlated random walk with move length and turning angle probability distributions [4]. The migration of living cells was exploited by Guttal and Couzin (2010) [18]. They developed an individual based model of movement and social interactions in a wide range of densities. A model for bird flocks built on empirical data and characterized the collective phenomenon was provided by Cavagna and Gardina (2014) [2].

Apart from these models, certain models which took the environmental factors into account developed. By combining analytic and numerical approaches, Pooley *et. al* (2007) studied hydrodynamic interactions of micro-organisms swimming at low Reynolds number [19]. Another study at the low Reynolds number limit came by Downton and Stark (2009) which proposed a method for a squirmer driven microparticle using stochastic dynamics [20]. Córdova-Figueroa and Brady (2008) developed a

model for self-propelled particles by suggesting a mechanism called "osmotic propulsion" [21]. With this mechanism the kinetic energy of the Brownian particles was transformed into mechanical motion. Yang *et al.* (2014) suggested a minimal model of two dimensional self- propelled repulsive particles in a box [22]. They also investigated the collective behaviour of particles for different densities. The transport and collective dynamics of dilute active suspensions simulated with thermal fluctuations by Wang and Duan *et al.* (2014) [23].

Although the Keller-Segel model was one of the earliest studies on collective behavior, it took decades for the topic to gain interest again. Schimansky-Geier *et al.* (1994) investigated the structure formation of active Brownian particles (ABP) by exploiting the ambiguity of diffusion process which could be considered as both microscopic and macroscopic [24]. A pioneering experimental study was contributed by Soni *et. al* (2003) which determined the correlative motion of colonial *Escherichia coli* in three dimensions [25]. Berke *et al.* (2008) showed both theoretically and experimentally that *E. Coli* bacteria were concentrated around the container walls [26]. Lately, many researchers were interested in collective behavior. Henkes *et al.* (2011) carried out a numerical study on dynamics of active particles with high concentration and with soft repulsive interactions in two dimensions [27]. Volpe *et al.* (2011) studied the motion of artificial microswimmers in patterned environment which contains intermittent obstacles [28]. Wang and Wolynes (2011) determined the spontaneous collective behavior of active matter systems via both anaytic and numeric methods [29].

A paper which considers chirality of microswimmers came out by Mijalkov and Volpe (2012) with their unique approach for active motion [3]. Dey *et al.* (2012) provided a study which considered the relationship between giant number of fluctuations of active matter in finite space and functions of structure formations in various models of active matter [30]. An experimental study on cluster formation on "gliding" bacteria was handed over by Peruani *et al.* (2012) [31]. The repulsively interacted active Brownian particles was considered by Stenhammar *et al.* (2013) and they presented a continuum theory for phase-seperation dynamics [32]. Palacci *et al.* (2013) built a system in which the propulsion of self-propelled particles can be turned on

and off with a blue light and showed that the existence of living crystals was related to far-from-equilibrium conditions [33]. Wang and Chen *et al.* (2014) investigated the transport and collective dynamics of dilute active suspensions with a simulation with thermal fluctuations [34]. A numerical analysis presented by Reichhardt *et al.* (2014) which was focused on the transport of interacting active run-and-tumble particles over disordered landscapes with obstacles [35]. A study on the phase diagram of purely repulsive, soft poly-disperse active particles in two dimensions, in a regime where the non-equilibrium effects were expected was provided by Filly and Henkes *et al.* (2014) [36]. Another recent experiment for characterizing the phase behavior and equation of state of a system of active colloids with sedimentation was made by Ginot *et al.* (2015) [37].

The unique property of self-propelling particles is that the system drives itself far from equilibrium. Since the equilibrium thermodynamics cannot be applied to the active matter systems directly, many researches has been focused on thermodynamic explanations. In 2008, Loi *et al.* showed that the effective temperature of active matter systems was compatible with the predicted result of the fluctuation-dissipation theorem [38]. Another study on the effective temperature of active matter was provided by Wang and Wolynes (2011) which stated that it depended on the susceptibility of the motors which was the internal mechanism of the active motion and Peclet number [29]. Nash *et al.* (2010) presented a simulation of run-and-tumble particles with far-field hydrodynamic interactions by lattice Boltzmann non-equilibrium steady states [39]. The equation of state of active particles was studied with a simulation by Mallory *et al.* (2014) and they found a dependence of pressure on the temperature and used this result to explain their anomalous behavior [40]. Filly and Baskaran *et al.* (2014) studied the dynamics of non-aligning and non-intetacting active particles in two dimensional containers and showed that the dynamical motion and thermodynamics of active particles were affected by boundaries [41]. A calculation for mechanical pressure of spherical active Brownian particles was presented by Solon *et al.* (2015) [42]. Lately, a comprehensive study by Takatori and Brady (2014) provided a generalization of thermodynamic concepts on active matter with the introduction of a new concept called “swim pressure” [43].

The collective behavior of macroscopic animals depends on the information transfer. Couzin *et al.* (2005) studied on a model in which the individuals who had the information of the required direction were not known by the other members of the community [44]. They also exploited the collective motion of such systems. Another study on information transfer presented by Sumpter *et al.* (2008) which showed that the procedure of information transfer was optimized when the density of animals was close to a phase transition between ordered and random motion [45].

Artificial microswimmers which can mimic the motion of active particles gained interest with latest advances in nanotechnology. Dreyfus *et al.* (2005) built a structure which consisted of a chain of magnetic particles linked by DNA. This structure could behave like a flagella, when it is attached to the red blood cell and if the magnetic field around it was changed [1]. In the same year, Dhar *et al.* (2006) provided study on autonomously moving nanorods which exploited the increase in the anomalous translational and rotational diffusion [46]. An experiment made by Howse *et al.* (2007) suggested the possibility of designing artificial chemotactic systems in which a chemical reaction catalysed autonomous propulsion [11]. The hydrodynamic interaction between two dumb-bells was studied by Alexander and Yeomans (2008) using analytic and numerical solution of Stokes' equation [47]. They investigated the interaction in which oscillating dumb-bells moved at low Reynolds number. Leonardo *et al.* (2009) showed the possibility of building a nano machine which could act as active particle when immersed into a bacterial bath [48]. Dunkel *et al.* (2010) presented a study for identifying the generic features of scattering of small particles from and artificial or natural microswimmer [49]. Another research by Putz and Dunkel (2010) tried to link the micro- and macro- behavior of individual organisms [50]. In order to mimic the collective spontaneous motion of hierarchically assembled living cells, Sanchez *et al.* (2012) used fabricated materials such as polymers and liquid crystals and found that at high concentration the created network would be the same for active matter [51].

Since there are huge number of publications on active matter researches, making a complete literature review is impossible. Other than the aforementioned studies, some novel works are summarized here: Reiman and Hanggi (2002) provided a good

introduction for the concept of Brownian motors and active Brownian motion [9]. In their comprehensive research, Takatori and Yan *et al.* (2014) presented the first publication which defines "swim pressure" [52]. Another study by Takatori and Brady (2014) analyzed the stress, dispersion, and average swimming speed of self-propelled particles subjected to an external field [43]. A numerical examination provided by Ray *et al.* (2014) on the force on active matter particles in Casimir geometries exploited the resemblance of Casimir effect [35]. Characteristics of active matter in low Reynolds number regime was exploited in an experimental study by Leoni *et al.* (2008) on a mechanism of pumping the fluid out of bacteria at low Reynolds number limit which induced its motion [53]. An impressive study on the hydrodynamics of a drop of active matter on a solid surface was presented by Joanny and Ramaswamy (2012) and they exploited the drop shapes with contractile and extensile stresses [54]. Selmeczi *et al.* (2008) provided a review of motile cell models which considered them as Brownian particles [8]. Also, theoretical works on active soft matter was collected in a review made by Marchetti *et al.* (2013) [55]. Another review focused on the swimming mechanisms of both biological and synthetic microswimmers and their individual and collective behavior came by Elgeti *et al.* (2015) [56].

In the microscopic world, the motion of a micron sized particle is dominantly affected by environmental factors which is not the case for macroscopic bodies. One of those phenomena is being at the low Reynolds number limit. The Reynolds number is defined as the ratio of inertial forces to viscous forces. This concept was devastatingly discussed by Purcell and the reader is referred to [57] for a further discussion. In summary, high Reynolds number limit resembles the validity of Newton's second law for the motion. That is, the movement is still affected by actual forces applied at a time before the motion takes place even though the net force on the particle vanishes. This means that forces could affect the motion in the future. However, for a body moving at low Reynolds number limit, the only responsibility for its motion goes to the forces acting on the particle at that very specific moment, not the forces acted in the past. For a better understanding, consider a human being swimming in a pool. The Reynolds number for this situation is approximately 10^4. This is a high value and one can neglect the viscous forces, cause the motion is not dominated by them.

In order to move a considerable amount, a little push from the environment would be abundant. On the other hand, a bacteria suspended in water experiences a Reynolds number about 10^{-4}, literally a low value and at that limit the inertial forces become negligible and play no role in the motion. Instead, the motion would abruptly stop if the bacteria stops pushing itself. The mathematical consequence of *the life at low Reynolds number* is that the inertial force term would be dropped from the equation of motion and the other forces on the particle could easily be handled.

Another effect in microscopic world is Brownian motion. When a micron sized particle, also called as *colloidal particle*, such as a pollen grain, immersed in water, the grain exhibits a peculiar behavior. This irregular action of pollen grains was first discovered by scottish botanist Robert Brown in 1827 [58]. The first implication he made was that grains showed the attitude because of their biotic nature. Nevertheless, when he repeated the experiment with inorganic matter, he observed the same motion and eliminated this conclusion. Also, the motion was still observable after the setup had been waited for a long time which suggested that the behavior was not resulted from a mechanical instability. Hence, the only possible explanation for the motion at hand was that the motion was purely caused by microscopic physical effects.

After Brown's discovery many physicists tried to shed light on the underlying condition of the Brownian motion. C. Wiener (1863) searched for an experimental evidence for the origin of the Brownian motion and found a connection between the motion and the molecules of the surrounding fluid [59]. Afterwards, an experimental study by M. Gouy [60] stated that a decrease in viscosity leaded to an amplification in the irregular motion. Theoretical studies which explained the origins and put the Brownian motion in a strong mathematical background were performed by Einstein [61,62], Smoluchowski [63], and Langevin [64]. According to these theories, Brownian motion was resulted from collisions between the particle and the constituting molecules of the immersing liquid whose motion was agitated by thermal fluctuations according to the laws of thermodynamics. The momentum exchange between particles in these elastic collisions causes the Brownian particle to displace randomly and the mean square displacement of individual particle increases with decreasing viscosity. Furthermore, since

the kinetic energy of particles increases with temperature according to equipartition theorem, the motion is amplified at higher temperatures.

Molecules of a liquid at a constant temperature move in an arbitrary manner because elastic collisions between individual particles randomizes their direction, hence momentum. A common assumption, though not analogous to the realistic cases, is that all the particles of the fluid should have the same kinetic energy. Although this assumption makes a considerable simplification for the theoretical studies, because of environmental factors and particle flow a non-uniform temperature gradient is present which leads thermal fluctuations across the liquid. Therefore particles do not always have the same speed, kinetic energy, and momentum. The differences in the direction and the amplitude of the momenta creates a net direction and amplitude in the momentum of the Brownian particle, but it changes infrequently. Brownian particles are approximately 1000 times larger than the particles of the medium which makes the momentum transfer from a molecule to the particle so low that the observation of a displacement would be impossible for an observable time scale. However, even for a considerably short observable time steps, the total number of collisions is always large (approximately 10^{12} collisions per second) [58]. So, the cumulative effect of these huge number of collisions makes the particle move and create opportunity for observation. Also, the direction of the motion would be random for different time steps since the transferred momentum comes with a randomized direction. The underlying physical mechanism of Brownian motion in this manner gave Einstein the idea of *random walks* [62]. By considering random walk theory, his theoretical interpretation wholly explains Brownian motion. Also, together with Smoluchowski's studies [63] and stokes' equation [58] which connects the viscosity and friction coefficient, Einstein found a relation between diffusion, viscosity, and temperature [62]. Hence, the microscopic and macroscopic consequences of Brownian motion were associated.

Brownian motion and diffusion could be explained with Einstein's theory but the problem about the dynamics of individual Brownian particles was still elusive. Individual dynamics was first studied by Langevin in 1908 which also presented the first stochastic differential equation [64]. In this theory, the motion of a Brownian

particle was determined by Newton's second law. The equation of motion contains an inertial term, a friction dependent dissipative term, also contains viscosity because of friction, and a *white noise* term which represents the irregular momentum transfer from surrounding molecules to the particle of interest. Because of being a balancing force equation, handling of any external potential was straightforward. Langevin equation is also significant for active matter modeling. Various models contain a Langevin-like equation for considering single particle dynamics. Moreover, it makes the numerical methods and simulation techniques easier.

Active matter in microscopic world also experiences Brownian motion. Like passive Brownian particles, the motion of an individual active particle is fluctuating, albeit it is not completely random. These fluctuations could be originated from certain environmental factors as well as internal effects brought about the resulting stochasticity of energy consumption process. The motion of macroscopic animals also exhibits randomness because of decision making process on which direction and/or speed would be chosen according to environmental factors and the motion of nearby individuals. The simplest way to consider such random fluctuations without examining their underlying mechanisms is to add a stochastic force term into the equation of motion. Thence, most of the active particle models are based on the concept of Langevin-like stochastic differential equation.

Active Brownian particles (ABP) is the term used for the Brownian particles that have an internal self-propelling mechanism. Schimansky-Geier *et al.* (1995) made the first study which introduces such term [24] as a reference for the Brownian particles which had ability to generate an active field in which a self-consistent motion took place. Following this work, self-driven particles who drive themselves far-from-equilibrium were called as "active Brownian particles" [17] [16] [28].

Many authors were interested in the individual behavior of ABPs. The main challenge in these studies was that while exploiting the properties of a single particle the collective behavior of a community such as swarming should also be concerned. The so called "Keller-Segel model" [13] and simulation study of Reynolds [14] had described

the particle behavior, however they were not well-equipped when it comes to explain the collective phenomena. A simple model which explained swarming behavior and applicable to both microscopic and macroscopic animals came by Vicsek in 1995 [15] (In the literature this model is usually called as *random walk model*, but throughout this document it will be mentioned as *Vicsek Model*). The model contains a simple position update term for individual particles which involves a velocity. The direction of this velocity is determined according to the average direction of nearby individuals with a small perturbation. In the original version of the model, the speed is constant for all the particles, however, it is possible to assign a different speed to each particle by using a probability distribution function. Despite its modesty, with certain modifications Vicsek model could explain collective behavior of various active systems.

Another model based on rotational diffusion was presented by Teeffelen and Löwen in 2008 [65]. One of the aforementioned crucial property of microscopic active matter is that particles predominantly exhibit Brownian motion. If their internal propulsion mechanism would somehow stop, the motion will completely turn into passive Brownian motion. Because of its extensive influence, this model sits on the similar grounds with Brownian motion. While particles experience random fluctuations, they are also subjected to rotational diffusion by which their orientation would be determined. Similar to the Vicsek model, positions of individuals regulated with a constant speed and a randomized direction. However, in contrast to the Vicsek model, the direction angle does not depend on other particles in the system, contrarily it is found via rotational diffusion constant. Single particle dynamics is perfectly described in Teeffelen model, but since their movement is completely independent of each other and because the environmental factors are not involved, the swarming behavior of active matter is not resolved.

Certain models of active motion take environmental factors into account that could affect the motion. This could be done by modifying the friction constant in the dissipative force term of the Langevin-like equation [66]. A commonly accepted form of the friction function is that it should depend on the velocity of the particle. Although this makes the solution of the equation harder, resulting simulations perfectly mimic

the actual situations. As a consequence of the method above, a model called *energy-depot model* was developed in order to express the behavior of an actively moving body in presence of localized energy sources which can be considered as food sources [16]. The presence of the food source attracts the particle and if the particle exhausts its internal energy before arriving at the source, its motion becomes passive Brownian.

The model used in this analysis is proposed as a hybrid one. In order to exploit swarming behavior and because of its simplicity, Vicsek model is chosen. However, since Brownian motion is so significant that cannot be neglected, it was necessary to integrate it. The numerical solution of simple Langevin equation provides the required displacement for Brownian motion for each time step. This displacement could easily be added to the positions of individuals in the Vicsek model. Also, the angular fluctuation of the orientation angle is calculated via the rotational diffusion. Thence, our analysis contains all the necessary effects and could be used as an alternative model.

Manipulation of ABPs under external fields would have significant consequences because it can be cooperated with the fabrication of micro- or nano- robots which could have usage in various areas. Acoustic fields could provide one of these external effects because they create a potential and particles experience force, so called *acoustic radiation force* (ARF). With acoustic fields, the motion of particles could be controlled in a contact-free way even in the microscopic scales [67]. Another technique for manipulating microscopic particles is optical tweezing.

Optical tweezers creates a harmonic potential fields around individual particles, and a single particle could be captured and manipulated in these types of fields. When subjected to a tightly focused laser light, the particles are trapped because of the forces of radiation pressure which arises from the momentum transfer [68]. A three dimensional harmonic trap is possible to be created with optical tweezers, since the radiation pressure results into gradient forces that pushes the particle into the point where the laser is focused. It is a commonly used technique in researches of soft matter physics in order to investigate of the properties of singular objects. Even though optical traps endanger the subjected entity, cause they may break the physiological structure

of it [69], together with acoustic fields, it can be used to select and extract a single particle from a whole bunch of community.

Acoustic radiation force was first discovered in 19th century and studied in detail for decades afterwards. Although the topic lost interest in the second half of the 20th century, the tendency to the acoustic radiation force increased again with the technological developments in the microfabrication techniques which made it possible to create microscopic acoustic sources. The first complete theoretical study on acoustic radiation forces was provided by L. V. King (1934) whereby incompressible particles suspended in an inviscid fluid were considered [70]. This study was widened into compressible particles by Yosioka and Kawasima in 1955 [71]. Subsequently, in 1962, Gor'kov generalized and simplified these works, yet it was limited to inviscid fluids [72]. The latest and the most powerful theory on acoustic radiation forces was presented by Settnes and Bruus in 2012 and their analytic method is summarized in Section 2.4 [67]. Since the addition of external fields to a Langevin-like equation is straightforward, its numeric solution for the position is also added to our hybrid model.

This study is devoted to the analysis of the behavior of active Brownian particles in presence of acoustic field. Manipulation of active particles with sound did not draw high attention, although there are two recent studies which consider the collective behavior of active matter in the presence of acoustic fields. Wang *et al.* (2015) [23] studied acoustic propulsion of artificial bimetallic micromotors and showed that acoustic forces could be used to reverse the direction of propulsion. Another study was provided by Takatori *et al.* (2016) [73] whereby they trapped active matter in a Gaussian acoustic profile and examined the collective behavior of the active particles. Albeit their novel approaches, these studies did not resolve the analytic form of the acoustic effects. Instead, acoustic fields were only used as harmonic potential sources for the sake of simplicity. In this study, the novel approach would be adding the analytic expression of the ARFs into the equation of motion of active Brownian particles. By characterizing the behavior of a single particle, the collective motion of a whole community could be resolved. Even though certain models are based on continuous dynamics of active matter and use hydrodynamic properties, these effects are not taken into account and

only individual dynamics is used in the analysis contained herein.

2. THEORETICAL BACKGROUND

An acceptable computer simulation of a physical system requires a well-behaved mathematical interpretation behind it in order to *mimic* a natural phenomena and create a virtual representation of the real world in which the laws of physics are always valid. In this context, understanding of the underlying theories is so important that they could be implemented accurately to the minimal portrayal.

The development of the theory of active Brownian motion starts with the traditional approach of passive Brownian motion and a Langevin-type equation. In this chapter, these two concepts are discussed as well as a theoretical study on ARF.

2.1. Brownian Motion

The discussion in the Chapter 1 stated that despite its early discovery, the Brownian motion had not been satiably explained for decades afterwards. In this respect, Einstein's theory of Brownian motion constitutes an important milestone in theoretical physics just as his other theories presented at the same time. His explanation was built upon two major postulates [61]:

(i) The underlying physical reason behind the motion is excessive impacts experienced by pollen grains. These impacts do not decay in time because the constituting molecules of immersing fluid regularly moves under the influence of thermal fluctuations.
(ii) Because of the complexity of the behavior of surrounding molecules, the motion could be explained in a probabilistic manner under the assumption that each impact is statistically independent.

Einstein's approach started the era of stochastic modeling in the analysis of natural phenomena because of its excellence, although the statistical descriptions were used in the context of thermodynamics before [74].

According to Einstein's theory [61], in one dimension (1D) the mean square displacement of a Brownian particle could be found as

$$\langle \Delta x^2 \rangle = 2D_T t \tag{2.1}$$

where Δx represents the displacement in x-direction, D_T is the translational diffusion coefficient, and $\langle\rangle$ denotes time average. The diffusion constant D_T comes from the probabilistic inference. In three dimensions (3D) this result could be generalized as

$$\langle \Delta r^2 \rangle = 6D_T t \tag{2.2}$$

in which Δr is given by $\sqrt{\Delta x^2 + \Delta y^2 + \Delta z^2}$. Then, the diffusion constant D_T is

$$D_T = \frac{\langle \Delta r^2 \rangle}{6\Delta t}. \tag{2.3}$$

The translational diffusion constant D_T can also be related to friction coefficient by using Smoluchowski equation [63]. Even though the Smoluchowski equation is similar to the convection-diffusion equation in fluid mechanics, it is different in a sense that it explains the flow of particles in vicinity of external forces acting on the system. To understand the relation, consider a measurable quantity whose concentration in the medium is given by a time independent function $C(x)$. Then, this function obeys the Smoluchowski equation of the form

$$D_T \frac{d}{dx} C(x) = \frac{1}{\gamma} C(x) F_{ext} \tag{2.4}$$

whereby γ characterizes the friction coefficient and F_{ext} is the total external force. With the definition of the work done on the system by external forces as $W = -\int F_{ext} dx$, the solution of this equation is simply given by

$$D_T \frac{ln[C(x)]}{ln[C(0)]} = \frac{-W}{\gamma}. \tag{2.5}$$

Then it yields the relation of concentration and work as

$$\frac{C(x)}{C(0)} = \exp(\frac{-W}{\gamma D_T}). \tag{2.6}$$

This relation defines a distribution function. The Boltzmann's distribution law should be valid for a system in equilibrium. Hence, the relation between the diffusion constant and friction could be easily inferred with the introduction of k_B as Boltzmann constant and T as the absolute temperature as

$$\gamma D_T = k_B T. \tag{2.7}$$

Equation (2.7) is the so-called *Einstein relation*. The relation connects the diffusion coefficient D_T which depends on the microscopic variables and the macroscopic measurable T [75].

The friction coefficient in the Equation (2.7) depends on the viscosity of the fluid and the characteristic dimension of the particle. For this constant George Gabriel Stokes expressed the formula for a spherical object of radius R flowing in a fluid of viscosity η at relatively low speeds without turbulence (i.e. at the low Reynolds numbers) which is given by the equation

$$\gamma = 6\pi\eta R. \tag{2.8}$$

Then substituting Equation (2.8) into Equation (2.7) yields the *Stokes-Einstein equation*

$$D_T = \frac{k_B T}{6\pi\eta R}. \tag{2.9}$$

For a fluid of viscosity η, Stokes-Einstein equation connects the diffusivity of a

spherical object with viscosity in the low Reynolds number regime.

Apart from the translational diffusion, particles also experiences sharp turns in their rotational motion which is called rotational diffusion. The rotational diffusion tensor for a spherically symmetric particle is given by [76].

$$D_R = \frac{k_B T}{8\pi\eta R^3}. \tag{2.10}$$

Unlike the translational diffusion, this is inversely proportional with R^3, hence it scales with the volume of the particle rather than the linear dimensions.

2.2. Langevin Dynamics

After Einstein's derivation, the individual dynamics of a single Brownian particle was presented by Langevin in which he used an "infinitely more simple" approach than Einstein [64]. What Langevin proposed was basically an application of Newton's second law to the forces acting on a single Brownian particle.

The equipartition theorem in statistical mechanics states that mean kinetic energy of a particle in 1D in thermal equilibrium should satisfy the condition

$$\langle \frac{1}{2} m v^2 \rangle = \frac{1}{2} k_B T. \tag{2.11}$$

where m is the mass and v is the velocity. There are two forces acting on the particle of mass m:

(i) *A viscous drag force* which is a basic hydrodynamic force and given by Stokes formula as $F_D = -6\pi\eta R dx/dt$ for a spherical particle at low Reynolds number.

(ii) *A fluctuating force* $\xi(t)$ which represents the impacts of the surrounding molecules on the particle. All that is known at this point is that it could be both positive and negative with equal probability, resembling that its mean value should be zero.

Thus the equation of motion for the particle can be found by writing the Newton's law:

$$m\frac{d^2x}{dt^2} = -6\pi\eta R\frac{dx}{dt} + \xi(t). \tag{2.12}$$

Multiplying both sides by x yields

$$\frac{m}{2}\frac{d^2}{dt^2}(x^2) - mv^2 = -3\eta\pi R\frac{d(x^2)}{dt} + \xi(t)x. \tag{2.13}$$

where $v = dx/dt$. Averaging over large ensemble of particles and substituting Equation (2.11) gives

$$\frac{m}{2}\frac{d^2}{dt^2}\langle x^2\rangle + 3\pi\eta R\frac{d\langle x^2\rangle}{dt} = k_BT. \tag{2.14}$$

The term $\langle\xi(t)x\rangle$ vanishes because x and $\xi(t)$ are independent functions and the mean value of $\xi(t)$ is zero. Then the general solution of the Equation (2.14) can be found by straightforward integration as

$$\frac{d\langle x^2\rangle}{dt} = \frac{k_BT}{3\pi\eta R} + C_0exp(\frac{-6\pi\eta Rt}{m}) \tag{2.15}$$

with C_0 is an arbitrary constant. The last term on the right-hand side is exponentially decaying and according to Langevin's estimation the time constant of the decay rate is of the order 10^{-8} s, shorter than any practically observable time, thus negligible. Therefore, integration with respect to the time gives the solution

$$\langle x^2\rangle - \langle x_0^2\rangle = \frac{k_BT}{3\pi\eta R}t \tag{2.16}$$

which corresponds

$$D = \frac{k_BT}{6\pi\eta R}. \tag{2.17}$$

This is the same result with Einstein's relation but from a completely different point

of view.

Langevin equation was the first example of stochastic differential equations because of the fluctuating force term $\xi(t)$. This term is also called as *the white noise*. Each solution of the Langevin equation represents a different trajectory. If one takes the average over a large ensemble of particles, the mean position would be zero. Despite there are several methods for solving these type of differential equations, this study only focuses only on numerical methods.

Even though the white noise was mentioned, it hasn't been discussed in detail yet. To exploit the properties of this function, a general form of the Langevin equation could be used:

$$\frac{dx}{dt} = a(x,t) + b(x,t)\xi(t) \tag{2.18}$$

where $a(x,t)$ and $b(x,t)$ are known continuous functions. The known nature of the white noise requires that for $t \neq t'$, $\xi(t)$ and $\xi(t')$ should be statistically independent. Moreover, because the functions $a(x,t)$ and $b(x,t)$ can absorb constant values, the mean value of white noise $\langle \xi(t) \rangle = 0$. These conditions require

$$\langle \xi(t)\xi(t') \rangle = g\delta(t - t') \tag{2.19}$$

where g is the strength. Equation (2.19) implies the correlation at different times does not occur and a non-realistic result that the variance of the white noise is infinite. The concept of infinite variance has no physical meaning, yet it could be idealized since statistically independent fluctuations in physical systems do exist.

The strength factor g could be found by considering a simple Langevin equation for a particle moving at the low Reynolds number. The dimensionless Reynolds number

is given by

$$Re = \frac{inertial forces}{viscous forces} \approx \frac{Rv\rho}{\eta} \tag{2.20}$$

For small scale biological applications its value is about 10^{-4}, resembling that the term md^2x/dt^2 is negligible. Then the Langevin equation can be written as

$$\frac{dx}{dt} = \frac{1}{\gamma}\xi(t). \tag{2.21}$$

All the symbols represents their usual meaning. Integration of this equation yields

$$x = x_0 + \frac{1}{\gamma}\int_0^t \xi(t^{'})dt^{'}. \tag{2.22}$$

Since the diffusion constant is related to run length of the particle (2.3), taking the square of both sides gives

$$(x - x_0)^2 = \frac{1}{\gamma^2}\int_0^t dt^{'}\int_0^t dt^{''}\xi(t^{'})\xi(t^{''}). \tag{2.23}$$

Taking the ensemble average, the run length could be found:

$$\begin{aligned}\langle x^2\rangle - \langle x_0^2\rangle &= \frac{1}{\gamma^2}\int_0^t dt^{'}\int_0^t dt^{''} g\delta(t^{'} - t^{''}) \\ &= \frac{g}{\gamma^2}\end{aligned} \tag{2.24}$$

From Equation (2.3), the run length should also be related to the diffusion coefficient. Thus, with also using Stokes-Einstein relation (2.9)

$$g = 2k_BT\gamma. \tag{2.25}$$

Given this so, the Langevin equation could be written in the form of

$$m\frac{d^2x}{dt^2} = -\gamma\frac{dx}{dt} + \sqrt{2k_BT\gamma}W(t) \tag{2.26}$$

in which a new function $W(t)$ is introduced which has zero mean and variance of

$$\langle W(t)W(t')\rangle = \delta(t-t'). \tag{2.27}$$

2.3. Active Matter

Active matter systems are constituted of individual self-propelled particles which can decide the direction of their movement. This ability is governed by the mechanism by which an individual could take up the ambient energy and convert it into kinetic energy, thus it gains a certain velocity and the system is driven far-from equilibrium. A wide variety of entities can be considered as active matter, ranging from flocks of bird to colonies of amoeba. Even though the collective behavior of these diverse entities looks similar, there are some basic differences between the movement mechanisms of individuals. For instance, both a bacterium and a bird experience irregular motion while they move, but this irregularity is mostly resulted from the Brownian motion for bacterium, while environmental factors and the communication with other members of community are dominantly responsible for the peculiar motion of bird. Because of this distinction, there were different models developed for each case. However, this study focused on two of them, Vicsek model and the model presented by Teeffelen and Löwen for ABPs.

2.3.1. Vicsek Model

Vicsek *et al.* [15] presented a model for the purpose explaining the phase transition of self-driven particles. However, their work was one of the pioneering studies on active matter whereby the swarming behavior was modeled with a simple but effective method. According to this model, each individual unit has a constant absolute *velocity*

whose direction is determined in consonance with the average direction of neighboring particles and a fluctuating term. In contrast to its simplicity, this model can be applied to many complex systems such as schools of fish, herds of animals, flock of birds as well as the motion of bacterial colonies in order to investigate their clustering, transport, and phase transitions.

The model provides the time evolution of the position of particles. According to it, the position of ith particle in 2D is determined by following equations:

$$\begin{aligned} x_i(t+1) &= x_i(t) + vcos(\theta(t))\Delta t \\ y_i(t+1) &= y_i(t) + vsin(\theta(t))\Delta t \end{aligned} \tag{2.28}$$

where x_i and y_i represents the x and y coordinates of the ith particle of the system, v is velocity, θ is the angle of the direction, and Δt is the time step as usual. The velocity v of particles is constant and same for all the particles in the ensemble. The time evolution of the direction angle $\theta(t)$ will be exploited from

$$\theta(t+1) = \langle\theta(t)\rangle_r + \Delta\theta \tag{2.29}$$

where the term with the subscript r represents the average direction of the particles in a circle of r centered at the ith particle. The last term $\Delta\theta$ gives randomization to the direction of the body. In their original paper, Vicsek *et al.* [15] suggested that it should be chosen from an interval of $[-\lambda/2, \lambda/2]$ in which the numbers are distributed with uniform probability. The number λ is one of the three free parameters of the system which represents the noise of the motion resulted from aforementioned environmental conditions. Other free parameters are ρ and v. ρ is the density which is given by N/L^2 where N is the number of particles in a box of length L. If the simulation would be performed in 3D, ρ should be turned into N/L^3. Furthermore, v is assumed to be constant in this analysis, however it is possible to change it regularly with a probability distribution which could resemble that particles move faster or slower in presence of energy sources and hazardous locations.

2.3.2. Active Brownian Particles

The motion of active Brownian particles is driven by random diffusion and an initial self-propelling force. The underlying mechanism of random diffusion part is the same as the passive Brownian motion for the particles of small sizes. The explicit form of the initial self-propelling force is not usually resolved in active matter models, however, some basic approaches could mimic the resulting effects of these forces on the body. The model presented by Teeffelen and Löwen [65] is used throughout this document even though it does not explain the collective behavior.

ABPs perform both the translational and rotational diffusion. Their directions are essentially chosen randomly under the effect of rotational diffusion. The translational Brownian motion arises with the diffusion constant given by Stokes-Einstein equation (2.9) as

$$D_T = \frac{k_B T}{6\pi\eta R} \tag{2.30}$$

where all the symbols have their usual meaning. Also, the rotational diffusion constant is given by Equation (2.10):

$$D_R = \frac{k_B T}{8\pi\eta R^3}. \tag{2.31}$$

The self-propulsion mechanism is added to the system by considering that each particle have a constant speed v whose direction is described by the particle orientation angle ϕ which will be determined by rotational Brownian motion. ϕ is also a coordinate like x and y so that it satisfies Langevin equation. Hence, by invoking the assumption

that the particles are spherical, the set of Langevin equations describing the motion is

$$\begin{aligned} \dot{x} &= vcos(\phi) + \sqrt{2D_T}W_x \\ \dot{y} &= vsin(\phi) + \sqrt{2D_T}W_y \\ \dot{\phi} &= \sqrt{2D_R}W_\phi \end{aligned} \tag{2.32}$$

where W_x, W_y, and W_ϕ are corresponding white noises. Since the motion takes place in the low Reynolds number regime, the inertial terms are neglected.

The ABP model and Vicsek model are represented in similar forms in a manner of numerical computation. Indeed, the difference between them is the direction of velocities. In ABP model, the direction angle is generated as Gaussian random number with a scale factor that depends on the rotational diffusion constant. This is the reason why collective behavior does not resolve in ABP model. On the other hand, the direction in Vicsek model depends on neighboring units. In the long run, the effect of the small perturbations disappears and all the particles in the community moves in the same direction.

2.4. Acoustic Radiation Force

The purpose of the study hereby is to manipulate the active Brownian motion of small particles with acoustic fields, and those particles move at the limit of low Reynolds number. Thus, inviscid theories cannot be used and a theory which considers the effect of viscosity is needed. Although there are many theoretical studies present for the physics of ARF, a recent approach by Settnes and Bruus (2012) [67] is the most suitable and contemporary one, and their work will be summarized here and used in the analysis contained herein.

Gor'kov (1962) stated that the acoustic radiation force could be determined as the time-averaged second order forces acting on a fixed surface [72]. The study of Settness and Bruus was based on this determination, however it is more accurate then previous versions of the same approach. Starting with the governing perturbation theory in

fluid mechanics whereby the density of fluid ρ, the pressure p, and the velocity of the medium v experience tiny perturbations, the second order forces could be calculated. Then the radiation force on the particle can be found as

$$\mathbf{F}^{rad} = -\int_{\partial\Omega} da([\frac{\kappa_0}{2}\langle p_1^2\rangle - \frac{\rho_0}{2}\langle v_1^2\rangle]\hat{\mathbf{n}} + \rho_0\langle(\hat{\mathbf{n}}.\mathbf{v}_1)\mathbf{v}_1\rangle). \tag{2.33}$$

Introduction of a time-harmonic velocity potential yields a considerable simplification in Equation (2.33). For a traveling velocity potential ϕ_{in} the acoustic radiation force could be written in the form of

$$\mathbf{F}^{rad} = \frac{4\pi}{3}R^3[\mathrm{Im}[f_1]\frac{\kappa_0}{2}\langle p_{in}^2\rangle + \mathrm{Im}[f_2]\frac{3\rho_0}{4}\langle v_{in}^2\rangle]\mathbf{k} \tag{2.34}$$

where κ_0 is the compressibility of the fluid, $\mathbf{k}$ is the wave vector, and f_1 and f_2 are monopole and dipole scattering coefficients.

The scattering coefficients f_1 and f_2 will be found by imposing the boundary conditions of a particle moving in a fluid of pressure p_1 and of velocity v_1 which are the first order corrections resulted from the perturbation theory of fluid mechanics. The first order scattering theory contains no coupling of these two coefficients, so they only represent the monopole and dipole scattering coefficients of outgoing wave.

The monopole coefficient f_1 can be found by using the conservation of fluid mass around the particle. On the other hand, the translational motion of the particle causes the velocity distribution of the fluid around it to be constructed according to particle velocity (no-slip boundary condition). This is the required boundary condition of determination of f_2. Hence, these two coefficients are found as

$$f_1(\tilde{\kappa}) = 1 - \tilde{\kappa} = 1 - \frac{\kappa_p}{\kappa_0}, \tag{2.35}$$

$$f_2(\tilde{\rho}, \tilde{\mu}) = \frac{2[1-\gamma(\tilde{\mu})](\tilde{\rho}-1)}{2\tilde{\rho}+1-3\gamma(\tilde{\mu})} \tag{2.36}$$

with $\tilde{\rho} = \frac{\rho_p}{\rho_0}$ and $\tilde{\mu} = \frac{\mu}{R}$.

The μ in the Equation (2.36) is called the thickness of the *the acoustic boundary layer* which is the thin region around the particle where most of the viscosity effects exist [77]. For a particle under the exposure of 1 MHz ultrasound wave the acoustic boundary layer thickness is

$$\mu = \sqrt{\frac{2\eta}{\omega}} \approx 0.6\ \mu m. \tag{2.37}$$

In summary, the resulting radiation force F^{rad} on a spherical particle of radius R, density ρ_p, and compressibility κ_p immersed in a fluid of density ρ_0, compressibility κ_0, and viscosity η and exposed to traveling acoustic wave is obtained as

$$\mathbf{F}^{rad} = \mathrm{Im}[f_2(\tilde{\rho}, \tilde{\mu})]\pi R^3 \rho_0 \langle v_{in}^2 \rangle \mathbf{k}. \tag{2.38}$$

In terms of acoustic energy density E_{ac}, the radiation force is given as

$$\mathbf{F}^{rad} = \pi R^3 k \mathrm{Im}[f_2(\tilde{\rho}, \tilde{\mu})] E_{ac} \hat{\mathbf{k}} \tag{2.39}$$

where k is the wave number.

3. METHODS

In presence of acoustic waves, small colloidal particles experience acoustic radiation forces. The analytic form and the magnitude of ARF change according the type of the acoustic waves which could be standing or traveling. Our purpose is to investigate the motion of active particles under traveling acoustic wave conditions. In order to do so, the Langevin equation which is discussed in Section (2.2) with an external force term could be used. Equations given in (2.32) are Langevin-type equations in low Reynolds number regime for active Brownian particles. Adding an external potential to these equations would be simple if a simulation on Equation (2.26) with an acoustic force could be handled. Therefore, the governing equation of this study could be written as

$$m\frac{d^2x(t)}{dt^2} = -\gamma\frac{dx(t)}{dt} + \sqrt{2k_BT\gamma}W(t) + F_{ext} \tag{3.1}$$

where F_{ext} is the external force and all the other symbols have their usual meaning. Each term in this equation will be solved numerically and the motion of an individual unit will be exploited and simulated.

Since Equation (3.1) is a *stochastic differential equation*, each solution of it represents a different path for the particle, making a general analytic solution tedious. However, this equation could easily be handled with numerical techniques and the trajectory of a single particle could be found in the form of a matrix.

Before diving into the numerical solution of the equation as a whole, the representation of the white noise via finite difference method should be investigated carefully.

3.1. Finite Difference Method

Finite difference method is commonly used numerical method in various applications of physics and engineering in order to solve the differential equations. It is

different from the standard calculus, because it depends on the *numerical evaluation* of functions with given discrete variable set. The standard calculus depends on *infinitesimal differentials*. In this aspect, the variable x of a given function $f(x)$ is continuous. However, if we discretize this variable as x_k $(k = 1, 2, 3, ..)$, the finite differences take place.

The method of finite differences is used to solve complex differential equations and yields a table of values for the functions in their discrete domains. On the other hand, a solution in closed form cannot be found. In order to understand the properties of this method, consider the Kepler problem for celestial objects. The two body problem the analytic solution is trivial and the equation of orbits can easily be found. However, if the number of bodies would be three or higher, the problem becomes almost impossible. With the method of finite differences, a simulation over N bodies could be done because it only calculated the points where each particle should be at a given time step, however, it does not yield a closed equation for orbits [78].

The basis of this method is to calculate the difference between two consecutive steps. This property makes it a perfect tool for approximation of derivatives, because according to the *mean value theorem* in differential calculus, there exists at least a point where the connecting line of each endpoints is parallel to the tangent [79]. The calculation of differences is straightforward. A function of a single variable x could be discretized by writing

$$\Delta f = f_k - f_{k-1} \tag{3.2}$$

where the indices k and $k-1$ represents the value of the function at the points x_k and x_{k-1}. Equation (3.2) is called the *backward difference* at the point x_k. There is also the method *forward difference* which could be written as

$$\Delta f = f_{k+1} - f_k. \tag{3.3}$$

These two methods gives the difference between the point of interest and the point before or after it. However, there is a symmetric method which is so-called *central difference*:

$$\Delta f = f_{k+1/2} - f_{k-1/2}. \tag{3.4}$$

Although the central difference seems more appropriate, non-integer indices may not be calculated for many cases. But, if one would like to calculate higher order differences, these non-integer indices become calculable in certain situations and the scheme would be more reliable, and in some cases, be more stable.

Apart from the schemes that constitutes the basic parts of an algorithm, an algorithm as a whole should be convergent and stable. Convergence means that a numerical solution of a differential equation should approach the true solution as the steps Δx, or Δt in case of time steps, goes to zero. Stability on the other hand, is that the small errors caused by perturbations in the numerical solution remain small and don't effect the final result. Since the techniques applied here are not complicated, the stability problem can be overcome by keeping the time step Δt of the algorithm smaller than the characteristic time of diffusion.

In this analysis, the backward differences is used because of its computational simplicity. Given well-established initial and boundary conditions, the solution would be always convergent, and necessary time steps can be exploited from theoretical studies. In this regard, the first derivative with backward differences is given by

$$\frac{dx}{dt} = \frac{x_i - x_{i-1}}{\Delta t}, \tag{3.5}$$

where x_i represents the position at the time t_i. Then, the second order derivatives could easily be found by taking the differences again as

$$\frac{d^2x}{dt^2} = \frac{x_i - 2x_{i-1} + x_{i-2}}{(\Delta t)^2}. \tag{3.6}$$

3.2. Simulation of White Noise

Finite difference method is useful for approximating derivatives. With its traditional approach Equation (3.1) can be used without the *white noise* term, $W(t)$. This is the most important term which gives the stochasticity to the Langevin equation and should be carefully considered. Various numerical methods were developed in order to treat this random term. The method proposed by Volpe and Volpe (2013) will be used in this document [80].

$W(t)$ is not continuous function. Its value changes for each value of t, even the step size Δt is so small. The properties of $W(t)$ can be summarized as follows:

(i) $\langle W(t) \rangle = 0$ for all t
(ii) $\langle W(t)^2 \rangle = 1$ for all t
(iii) $W(t_1)$ and $W(t_2)$ are independent of each other when t_1 is different than t_2 [81].

These properties make the application of finite difference method impossible to $W(t)$ for the reason that the approximated values at t_i are wildly distinctive due to lack of continuity and infinite variation. For the sake of understanding of the behavior of this function within the approach of finite differences, a simplified equation of Brownian motion, usually called *random walk*, can be used:

$$\frac{dx}{dt} = W(t). \tag{3.7}$$

This equation generally represents *free diffusion*. For applying a numerical method to this equation, a sequence of random numbers W_i which discretizes $W(t)$ and imposes its properties is necessary with the following conditions:

(i) The mean of W_i must be zero because both the positive and negative numbers should be equally probable.
(ii) Their variance should be $1/\Delta t$ (As discussed in Section (2.2), the variance of

$\langle (W_i \Delta t)^2 \rangle$ should be 1 cause it must be an integrable quantity).

(iii) Any two values W_i and W_j at two different times t_i and t_j should be statistically independent of each other.

As a computational shortcut, a Gaussian number set w_i with zero mean and unit variance could be used and by re-scaling, the properties mentioned above could be imposed as

$$W_i = \frac{w_i}{\sqrt{\Delta t}} \tag{3.8}$$

Thus, application of finite difference method to the Equation (3.7) gives

$$\frac{x_i - x_{i-1}}{\Delta t} = \frac{w_i}{\sqrt{\Delta t}}, \tag{3.9}$$

and leaving x_i alone in the left-hand-side in order to make it explicitly calculable

$$x_i = x_{i-1} + \sqrt{\Delta t} w_i. \tag{3.10}$$

An application of Equation (3.10) is provided in Figure (3.1) which shows the trajectory of a particle making random walk in 2D with the time step $\Delta t = 0.1\ s$.

In many areas of computational physics, the stability and convergence of an algorithm mostly depends on the value of characteristic time scale. If Δt is much greater than the characteristic time scale of the system, the numeric solution would diverge or yield non-physical situations because of the unstability. However, the random walk equation has no characteristic time, leading the algorithm to be inherently stable.

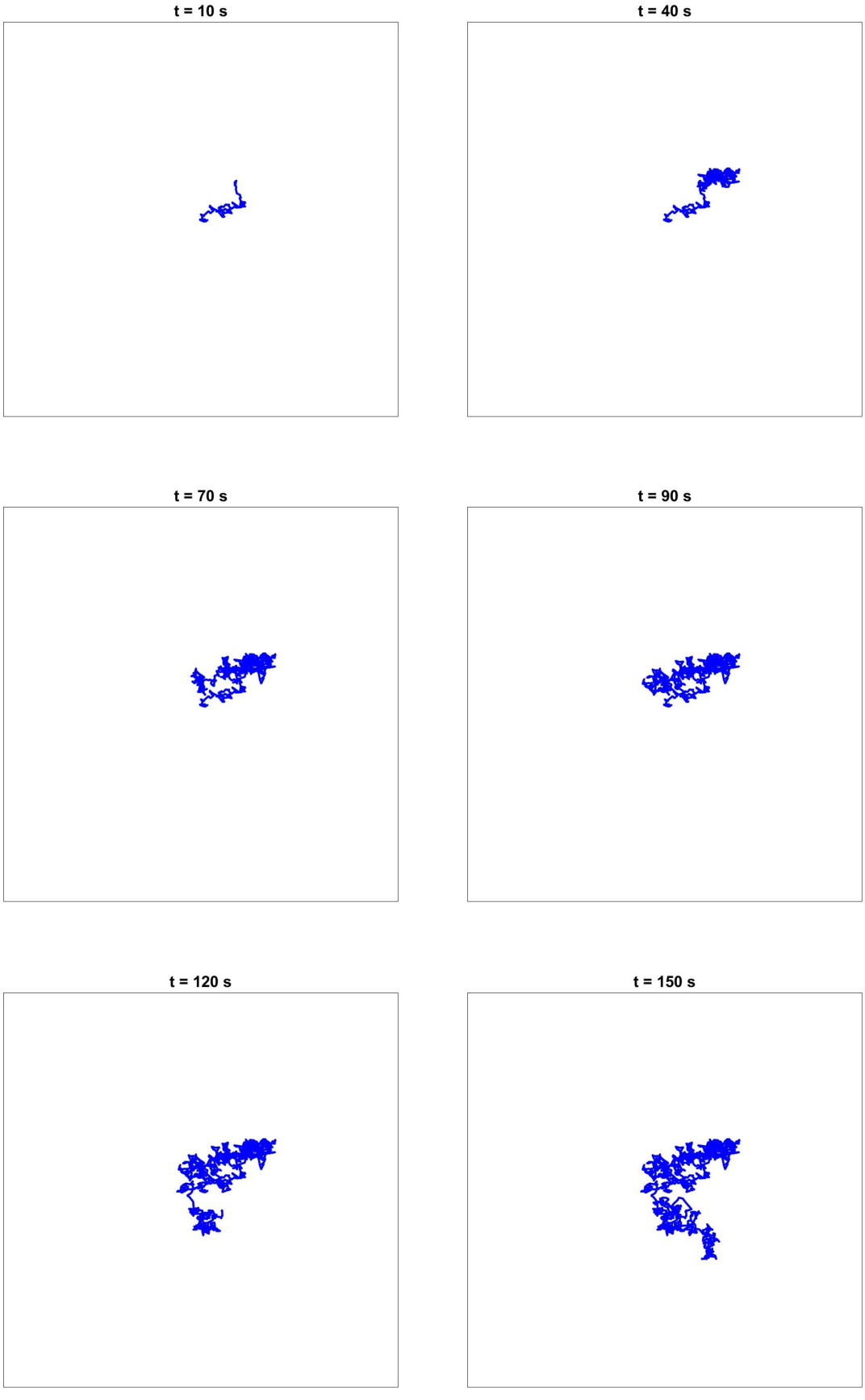

Figure 3.1: Simulation of random walk in two dimensions with $\Delta t = 0.1$ s

3.3. Simulation of Brownian Motion

In consideration of Brownian motion of real particles, it would be beneficial to understand which processes the particle undergoes in a submerging fluid. The collisions between the particle and the molecules of the surrounding medium lead the particle to experience *diffusion*. These collisions are also responsible of amending the velocity of the particle which is adequately randomized after each successful time step. The underlying mechanism of Brownian motion is discussed in Chapter (1) and theoretical studies are summarized in Chapter (2). The equation of interest for the Brownian motion developed in preceding chapter is then given as

$$m\frac{d^2x}{dt^2} = -\gamma\frac{dx}{dt} + \sqrt{2k_BT\gamma}W(t). \tag{3.11}$$

The methods provided in Sections (3.1) and (3.2) shows how to treat the derivatives and white noise terms. By importing equations (3.5) and (3.6) for the derivatives and (3.8) for the white noise to the Langevin equation, the numerical solution could be found as

$$m\frac{x_i - 2x_{i-1} + x_{i-2}}{(\Delta t)^2} = -\gamma\frac{x_i - x_{i-1}}{\Delta t} + \sqrt{2k_BT\gamma}\frac{w_i}{\sqrt{\Delta t}}. \tag{3.12}$$

Summing up the terms and leaving x_i alone on the left-hand-side yields an explicit scheme:

$$x_i = \frac{2 + \Delta t(\gamma/m)}{1 + \Delta t(\gamma/m)}x_{i-1} - \frac{1}{1 + \Delta t(\gamma/m)}x_{i-2} + \frac{\sqrt{2k_BT\gamma}}{m(1 + \Delta t(\gamma/m))}(\Delta t)^{3/2}w_i. \tag{3.13}$$

At a first glance, one may think that this scheme would be hard to implement because of the terms x_{i-1} and x_{i-2}. However, with convenient boundary and initial conditions these terms would be easy to care about and the time evolution of the position would be calculated.

The ratio $\tau = \gamma/m$ is the momentum relaxation time and it defines the charac-

teristic time of the diffusion which is also the necessary time in which the effects of the inertial momentum would be negligible compared to the random momentum transferred from immersing molecules to the particle in the low Reynolds number regime [80]. Thence the inertial term in Equation (3.11) could be considered as negligible. Then, with the help of Einstein relation (2.7), Equation (3.11) turns into a simpler version

$$\frac{dx(t)}{dt} = \sqrt{2D_T}W(t). \tag{3.14}$$

Application of techniques yields

$$x_i = x_{i-1} + \sqrt{2D_T\Delta t}w_i. \tag{3.15}$$

For long time steps ($\Delta t \gg \tau$) that is at low Reynolds number which is the situation of interest for the analysis herein, Equation (3.14) provides a superb approximation to Brownian motion, yet for short time steps it presents clear deviations from desired results and the inertial term should be preserved.

A sample simulation carried out according to Equation (3.15) within a box of 30 $\mu m \times 30$ μm in 2D with temperature $T = 300$ K, particle radius $r = 1$ μm, and the time step $\Delta t = 0.01$ s is provided in Figure (3.2). The blue line in the figure represents the path of the center of mass of the particle.

3.4. Simulation of Active Brownian Motion

The numerical solution of general Langevin equation (3.1) without the external effects shows the proper behavior of a passive Brownian particle and can be used in simulations. Starting with this solution, the active attitude can be described in a similar manner. As depicted in the Section (2.3), there are two basic models on which this study focused. Both of these models have a constant velocity term whose direction is somehow randomized or specified.

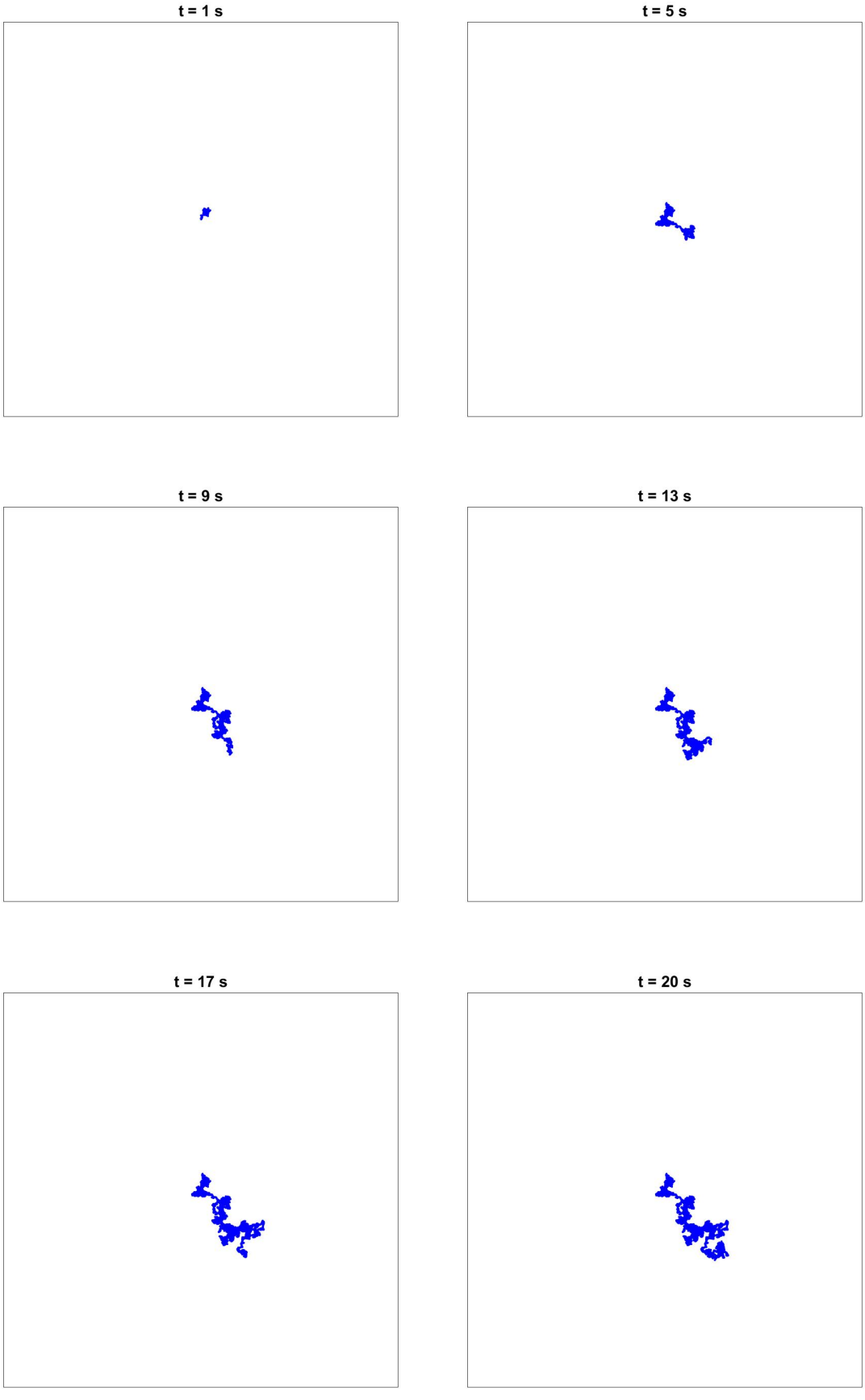

Figure 3.2: Simulation of a single Brownian particle

3.4.1. Vicsek Model

The model presented by Vicsek *et al.* (1995) provided a simulation tool for active matter which considered the swarming behavior [15]. Even though it did not contain a closed formula for the motion, it resembles the numerical solution of a non-stochastic equation of motion.

Vicsek model was based on a set of equations given in Equations (2.28) and (2.29). Those equations are written in the form of *forward differences*. In order to be consistent, they should be written in the form of *backward differences* as:

$$\begin{aligned} x_i &= x_{i-1} + vcos(\theta_i)\Delta t \\ y_i &= y_{i-1} + vsin(\theta_i)\Delta t \end{aligned} \tag{3.16}$$

and the direction is written as

$$\theta_i = \langle \theta(t) \rangle_r + \Delta\theta \tag{3.17}$$

with all the symbols having aforementioned meanings.

An implementation of this model is given in Figure (3.3) with the parameters $r = 2\ \mu m$, $\rho = 1000\ kg/m^3$, $N = 500$, $T = 300\ K$, and $v = 5\ \mu m/s$.

Since the original Vicsek model does not contain the Brownian motion, it is necessary to modify the Equation (3.16) in such a way that it includes Brownian part. In order to do so, a combination of Equation (3.15) with Equation (3.16) could be used. The behavior of Brownian motion is described by the term $\sqrt{2D_T\Delta t}w_i$. Since this term represents the irregular position change, it can be added to the governing Vicsek equations as

$$\begin{aligned} x_i &= x_{i-1} + vcos(\theta_i)\Delta t + \sqrt{2D_T\Delta t}w_i \\ y_i &= y_{i-1} + vsin(\theta_i)\Delta t + \sqrt{2D_T\Delta t}w_i \end{aligned} \tag{3.18}$$

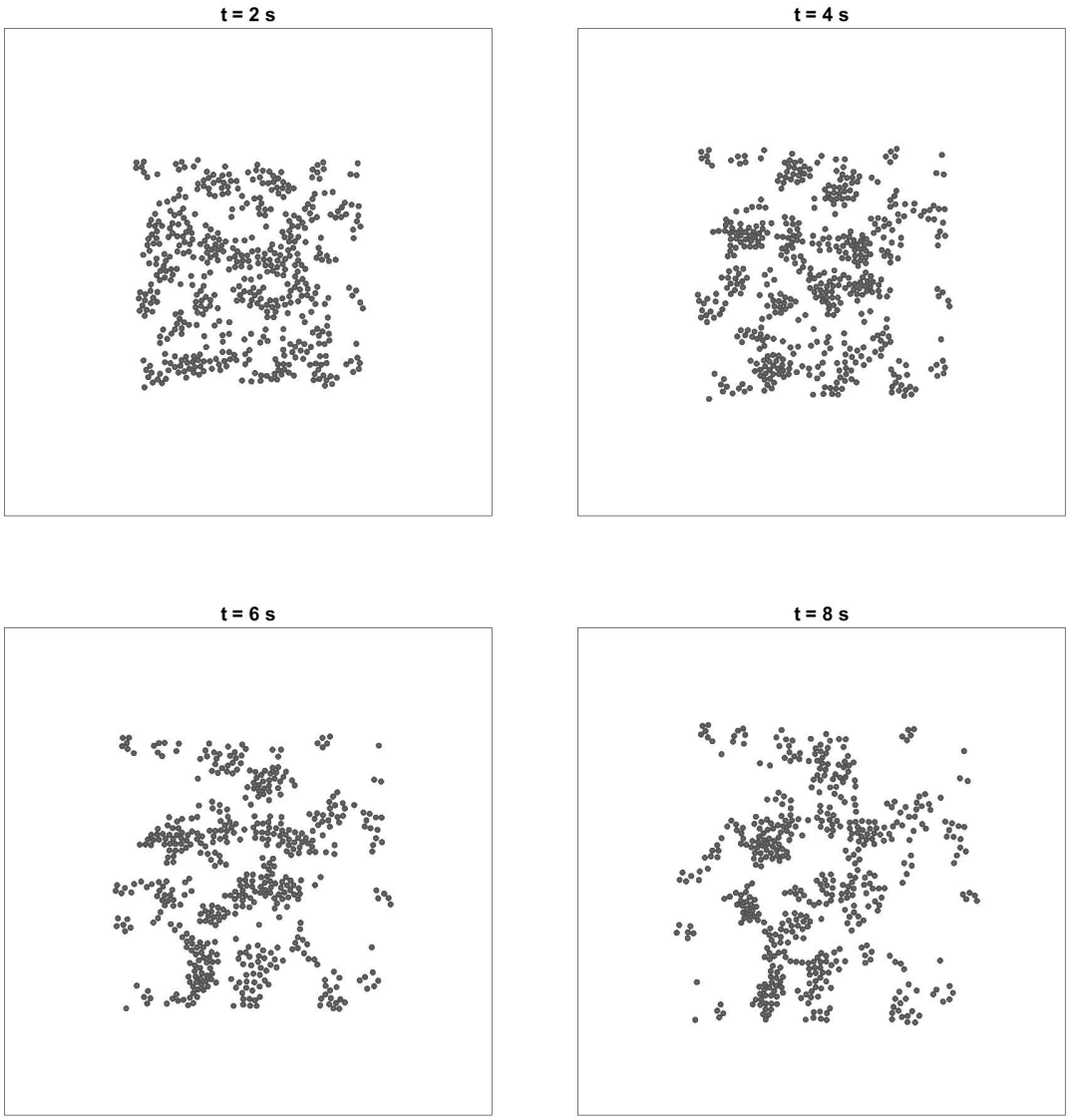

Figure 3.3: Simulation of Vicsek model with 500 particles. The dimensions of the box are 250 $\mu m \times 250$ μm.

assuming the diffusion constant D_T is the same for both x and y dimensions. This is a hybrid equation containing both the swarming and diffusive behavior.

3.4.2. Active Brownian Particles

Vicsek model is suitable for active motion because it exploits the collective behavior in animal groups. However, it does not resolve the Brownian properties of active motion. Therefore, another model provided by Teeffelen and Löwen (2008) is also used in this analysis (explained in the Section (2.3) [65]).

The equation set given for this model (2.32) yields a clear deviation from Vicsek model in a manner that the direction of particles would be determined via their rotational diffusion. With the numerical techniques developed in sections (3.1) and (3.2), the governing equations of the ABPs could be written as

$$\begin{aligned} \frac{x_i - x_{i-1}}{\Delta t} &= vcos(\phi_i) + \sqrt{2D_T}\frac{w_x}{\sqrt{\Delta t}}, \\ \frac{y_i - y_{i-1}}{\Delta t} &= vsin(\phi_i) + \sqrt{2D_T}\frac{w_y}{\sqrt{\Delta t}}, \\ \frac{\phi_i - \phi_{i-1}}{\Delta t} &= \sqrt{2D_R}\frac{w_\phi}{\sqrt{\Delta t}} \end{aligned} \tag{3.19}$$

where w_x, w_y, and w_z are Gaussian random numbers. Writing the ith terms explicitly yields similar equations with Vicsek model:

$$\begin{aligned} x_i &= x_{i-1} + vcos(\phi_i)\Delta t + \sqrt{2D_T\Delta t}w_x, \\ y_i &= y_{i-1} + vsin(\phi_i)\Delta t + \sqrt{2D_T\Delta t}w_y, \\ \phi_i &= \phi_{i-1} + \sqrt{2D_R\Delta t}w_\phi. \end{aligned} \tag{3.20}$$

An application of this model for a single particle of radius $r = 2\ \mu m$ is provided in Figure (3.4). Each plot shows the trajectory of center of mass of the particle after the time of 10 s for different values of speed v. The simulation was carried out for four times and each of which was represented with a different color. Figure (3.5) shows the

simulation of a collection with 500 particles with $r = 2\ \mu m$ and $v = 5\ \mu m$. All the other parameters are the same as Figure (3.3).

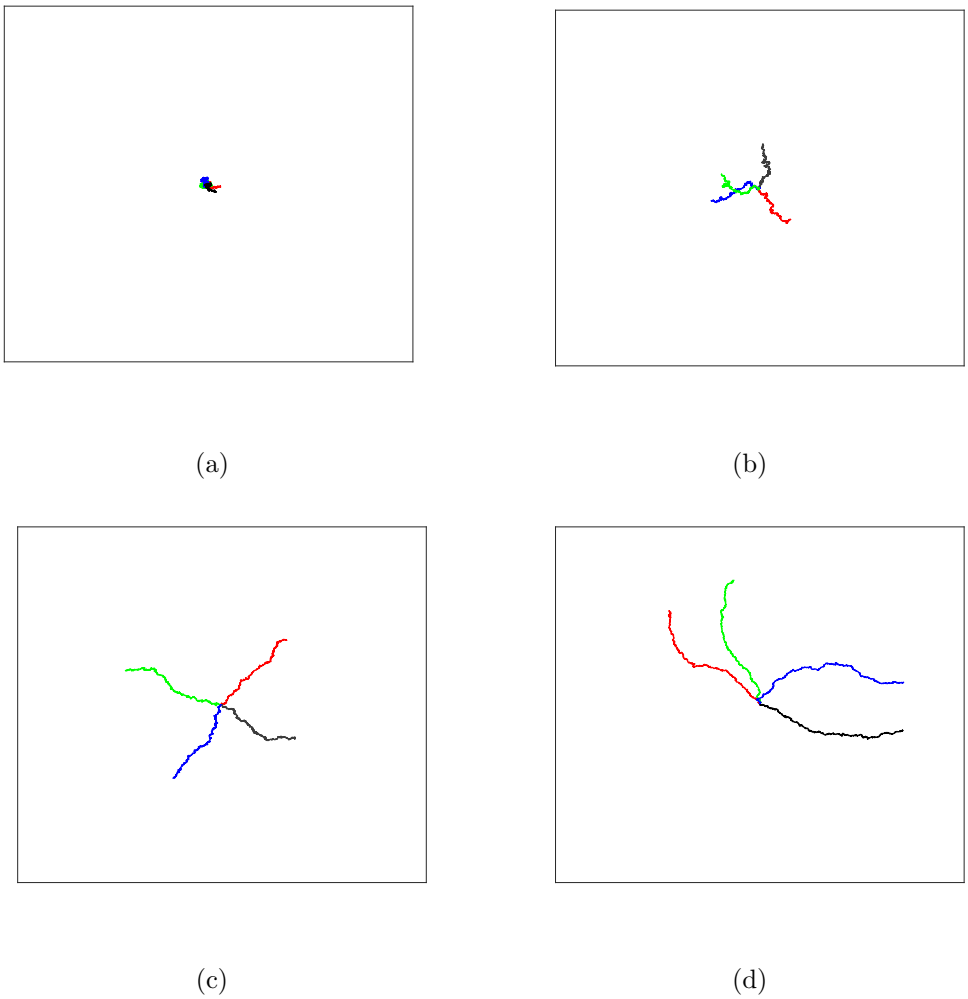

(a) (b)

(c) (d)

Figure 3.4: Simulation of a single active Brownian particle according to the model provided by Teffelen *et al.* (2008) for different values of v. The dimensions of the box are $40\ \mu m \times 40\ \mu m$ each line shows a different trajectory of center of mass of a particle of radius $r = 2\ \mu m$ initially placed at the center. The different values of v are in (a) $v = 0$ (passive Brownian motion), (b) $v = 1\ \mu m$, (c) $v = 2\ \mu m$, and (d) $v = 3\ \mu m$.

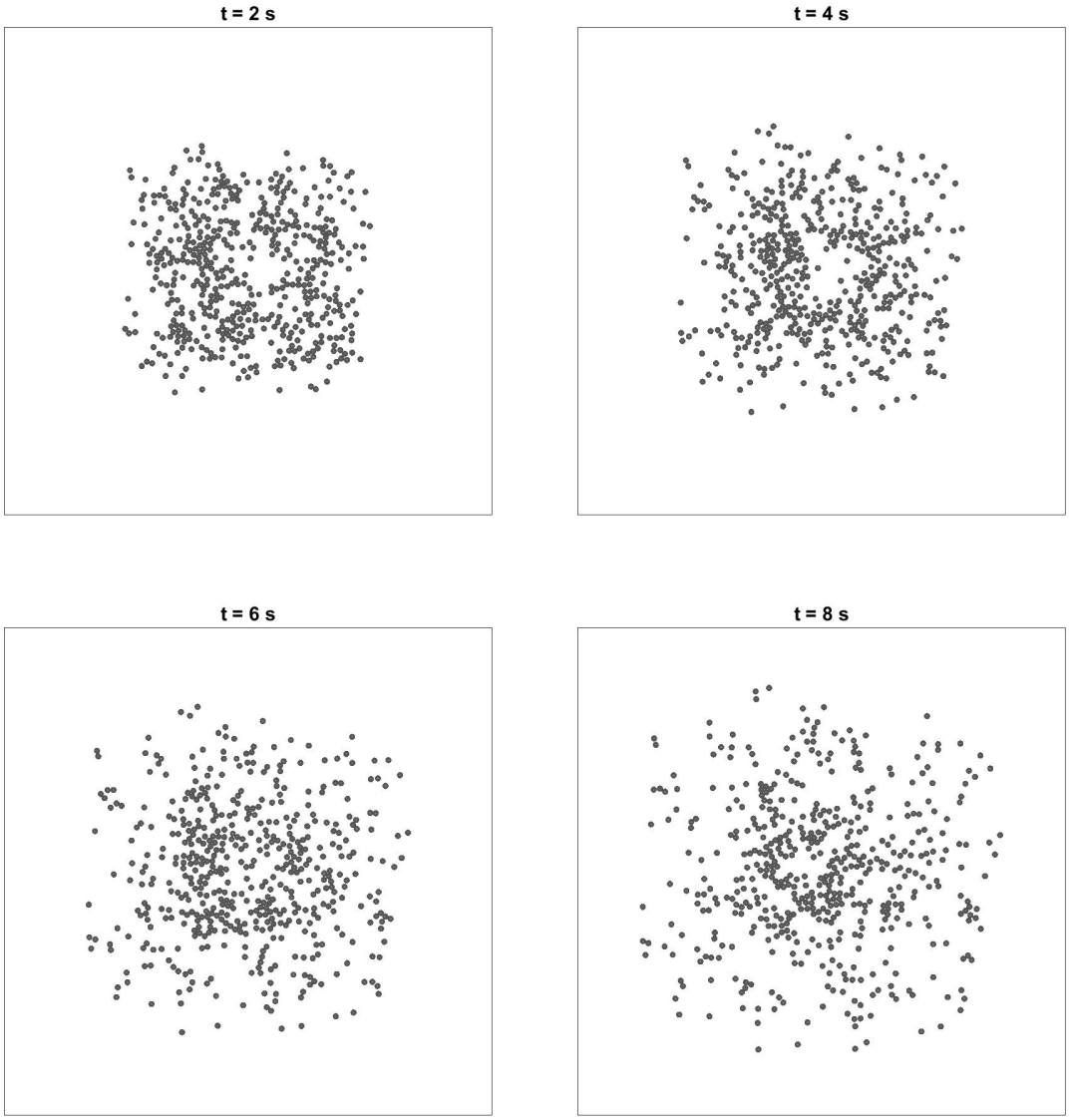

Figure 3.5: Simulation of ABP model with 500 particles

3.5. Acoustic Force on a Single Active Brownian Particle

External effects could be added to the generic Langevin equation as given in Equation (3.1). The last term in that equation arises from the external forces. In an acoustic field according to the discussion in the Section (2.4), the resulting acoustic force on a particle is given as [67]

$$\mathbf{F}^{rad} = \pi R^3 k \mathrm{Im}[f_2(\tilde{\rho}, \tilde{\mu})] E_{ac} \hat{\mathbf{k}}. \tag{3.21}$$

This term contains neither position nor time dependence, so it can be treated as constant throughout the medium.

The inertial term md^2x/dt^2 can be neglected in Equation (3.1) because of the low Reynolds number limit. Then applying numerical techniques to it gives

$$\frac{x_i - x_{i-1}}{\Delta t} = \sqrt{2\frac{k_B T}{\gamma}} \frac{w_i}{\sqrt{\Delta t}} + \frac{F^{rad}}{\gamma}. \tag{3.22}$$

Rearrangement of terms yields

$$x_i = x_{i-1} + \sqrt{2 D_T \Delta t} w_i + \frac{D_T}{k_B T} F^{rad}. \tag{3.23}$$

Hence, any constant external force effects the position with a scale factor of D_T/kT. If the force had dependence of position and/or time, the integration of it would require so much effort and different techniques.

In order to see the effect of ARF, a simulation of a single passive Brownian particle with radius $r = 2\ \mu m$ in presence of optical traps would be appropriate. Figure (3.6) shows the simulation. ARF starts to act on the particle at $t = 5\ s$. Before that time, the particle sits in the center of its motion, however, after the force is applied, a clear deviation is observed in its mean position.

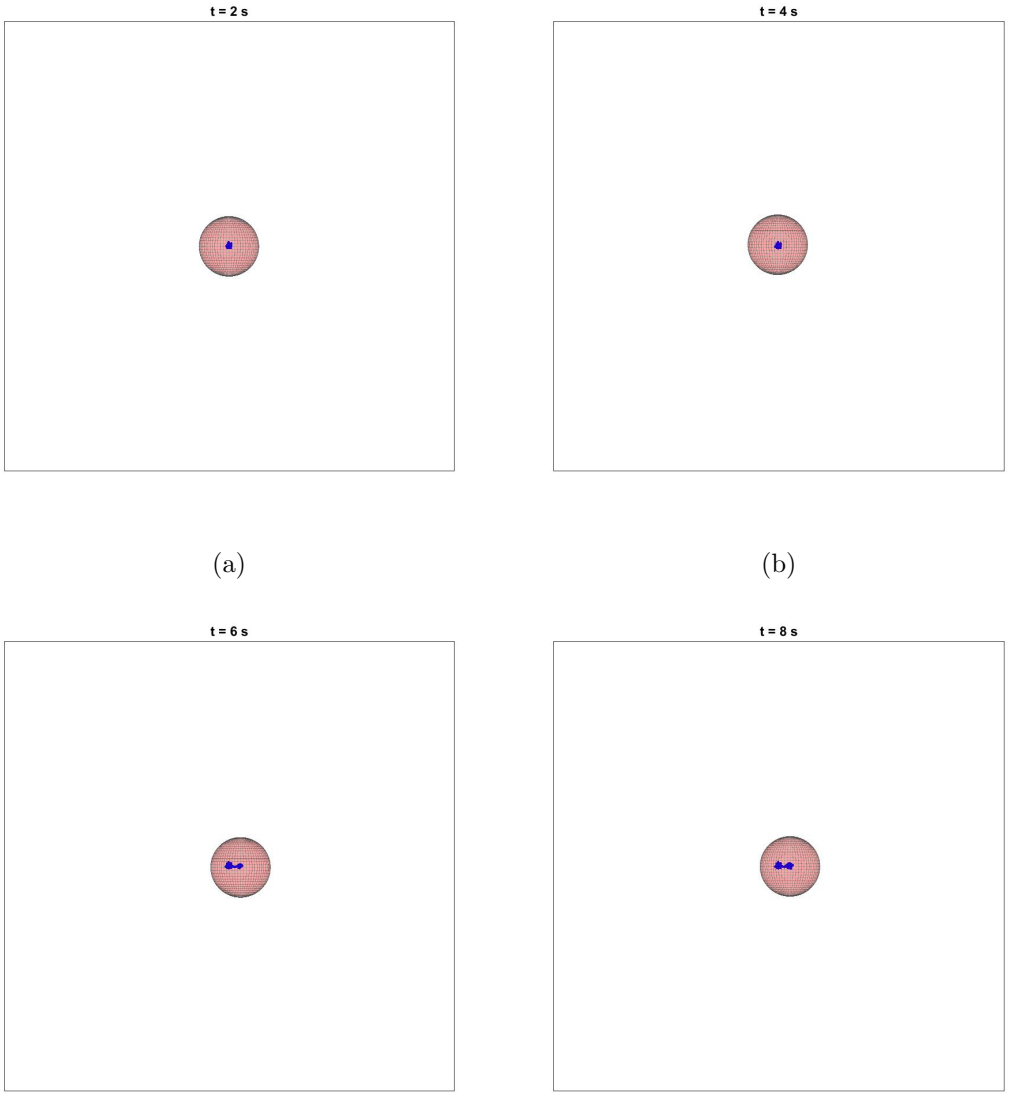

Figure 3.6: The effect of ARF on a single Brownian particle which is trapped by an optical tweezers. (a) and (b) shows the captured particle. At $t = 5\ s$, the force is applied and deviations from the center is observed in (c) and (d).

3.6. Optical Traps

Optical traps can be used to capture individual particles in a crowded environment. Even though it is a consequence of the gradient forces resulted from the radiation pressure, the effect of optical tweezers could be represented primitively as Hooke's law [80]:

$$F_{trap} = \kappa_{trap}\Delta x. \tag{3.24}$$

The Δx is the distance of the particle to the center of the trap and the κ_{trap} in Equation (3.24) is the trap stiffness. The value of stiffness depends on many parameters such as surface properties of particle, radius, numerical aperture of the objective, intensity and color of laser radiation, and the orientation of the equipment. It could have different values in all three dimensions, however, in planar dimensions where the laser light makes a perpendicular angle, the stiffness is uniform. In the third dimension, the stiffness is usually different and lower than the ones in other two dimensions since the radiation pressure is less effective.

The calculation of the trap force would be different than the one for ARF, because its value depends on the position. For a problem which involves only optical trap and Brownian motion, the equation motion would take the form

$$m\frac{d^2x}{dt^2} = -\gamma\frac{dx}{dt} + \kappa\Delta x + \sqrt{2k_BT\gamma}W(t) \tag{3.25}$$

with all the symbols having their usual meanings. The term Δx contains the current position x of the object and the position in which the trap is centered. So, with the low Reynolds number approximation, application of finite difference gives

$$x_i = x_{i-1} - \frac{\kappa}{\gamma}(x_i - P_{trap})\Delta t + \sqrt{2D_T\Delta t}w_i \tag{3.26}$$

where P_{trap} is the point of the trap center. The solution of this equation as a whole

is not needed. It can be solved by taking care of the trap force in every time step, then adding it as a constant force. The crucial part is that the range of trap should not be extremely large. In reality, a single optical trap can only capture one particle. Therefor, the general assumption for the trap range is between $1.5r$ and $3r$ and it could be changed by arranging laser parameters.

A comparison of optical traps and Brownian motion is provided in Figure (3.7) which shows the particle and its center of mass' path with a blue line with and without the optical tweezers. As it can be clearly depicted from the simulations, optical traps "restricts" the particle in a harmonic trap.

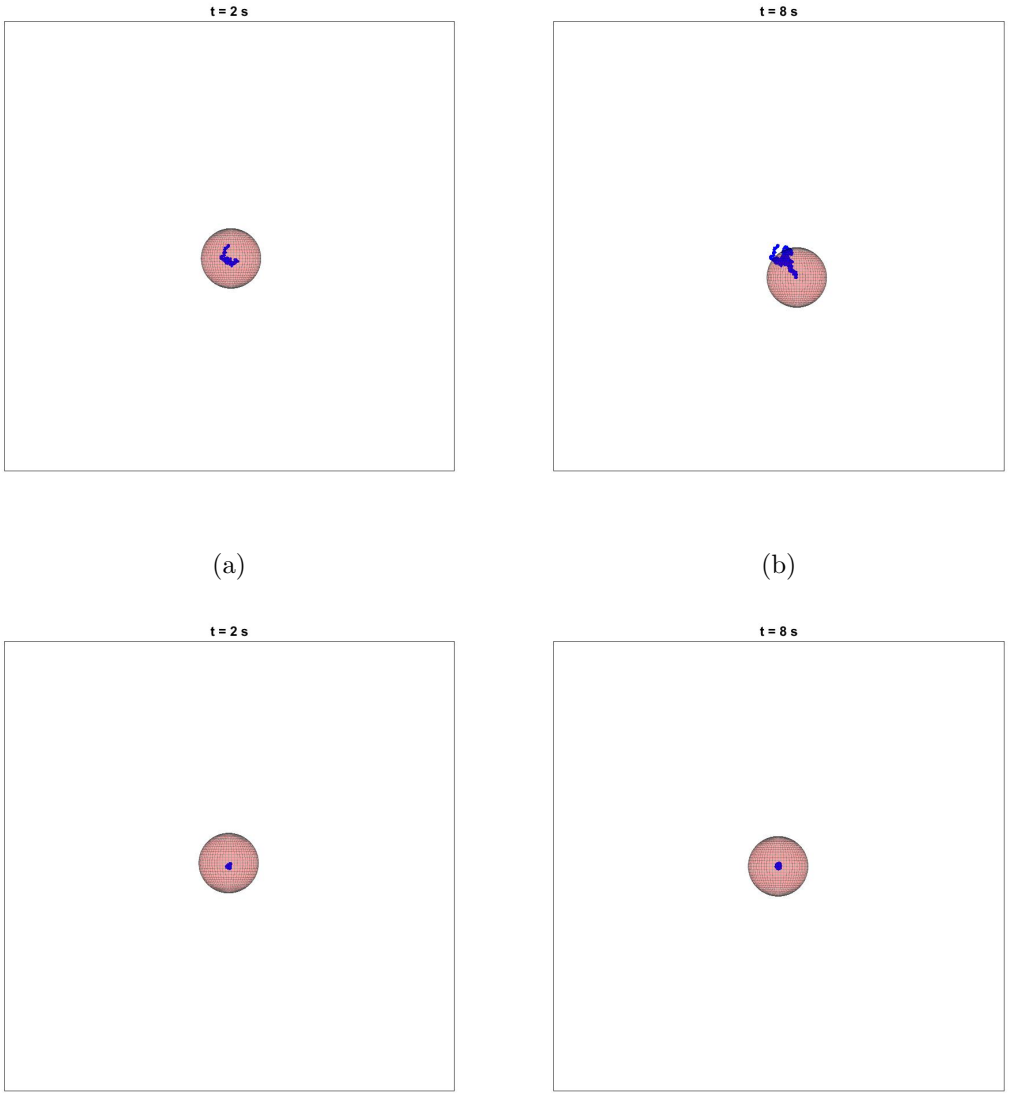

Figure 3.7: The effect of optical trap. The particle with $r = 2\ \mu m$ makes Brownian motion in (a) and (b). (c) and (d) show the same particle under the same environmental conditions captured by the optical trap. The blue line shows the trajectory of the center of mass, as usual.

4. RESULTS

The motion of microscopic active matter can be controlled and guided by using acoustic wave fields. It has long been known that in presence of acoustic waves, small particles suspended in a viscous fluid would experience the so-called *acoustic radiation forces*. Even though there is no net flow created inside the fluid, suspended particles can move under the effect of ARF. Both standing and traveling waves can be created with acoustic waves. Standing waves cause gradient forces which lead particles to be trapped around the wave nodes. On the other hand, only constant forces across the fluid can be created by traveling waves. This study is focused only on traveling waves.

An important feature of traveling acoustic waves is that for an inviscid bulk, the ARF on particles is zero [82]. This result could be exploited from Figure (4.2) which shows the relation between the temperature and ARF. For an acoustic field of frequency 1 MHz, ARF on a particle suspended in water decreases as the temperature increases. This trend continues for the higher values of temperature which lead lower viscosity values. For active Brownian particles, the effect of viscosity cannot be neglected because of the low Reynolds number regime. Therefore, the particles can be easily manipulated with the sweeping effect of the ARF. However, this case is not true for all active Brownian particles. Settnes and Bruus (2012) stated that most of the viscosity effects happens inside the distance of 5μ from the outer shell of the particle [67]. Beyond this limit, the fluid can be treated as inviscid. Also, the radius of the particle should be comparable with the thickness of the acoustic boundary layer μ which is about 0.6 μm in water for the field of frequency 1 MHz. Under these circumstances, particles with radii bigger than 3 μm do not affected by a traveling wave. The simulations here were performed for the particles of radius 2 μm.

The value of ARF mostly depends on two parameters. The first one is the viscosity, the effect of which is already discussed above. Another parameter is the frequency. The frequencies of acoustic waves which can be produced experimentally covers a wide range, starting from a few Hz and goes up to the order of GHz. Widely used acoustic

transducers can generate waves in KHz and MHz ranges. The value of the force in this frequency window for the temperature of $25°C$ is provided in Figure (4.1). The peak value of the force is between 170 MHz. Above this value, even though there is not a strong decrease, there are small changes in the force. This behavior is also seen in Table (4.1) and (4.2) for different values of frequencies.

The position of the peak value of ARF in the Figure (4.1) is determined by two different parameters which are the radius R of the particle and the density ratio $\tilde{\rho}$. With the increasing density ratio $\tilde{\rho}$, the peak frequency decreases as given in the Figure (4.3). Also, denser particles experience higher peak forces, despite the lower values of forces for low frequencies (Figure (4.4)). Moreover, Figure (4.5) shows the relation between the peak frequency and the radius of particles. As discussed earlier, in order the ARF for a traveling wave to be present, the particle radius should be smaller than 3 μm. This makes the chosen range of radii reasonable. It is an interesting fact that the peak forces of bigger particles occur in lower frequencies. Even though it is not explicitly showed in the analytic form of the ARF, it is a general fact that the resonance frequencies of larger particles are lower, and the acoustic effects are maximized when the frequency of the acoustic wave is close to the resonance frequency of the particle. Our results are in agreement with this fact.

The analytic expression of ARF could be integrated with the equation of motion of an individual particle, that is a Langevin-like equation, and its effect on the behavior of the particle can be exploited. With this method, the collective behavior of an active particle community could also be investigated.

From now on, all the simulations are performed with parameters of the density of the medium $\rho = 1000\ kg/m^3$, the temperature $T = 5\ C$, the kinematic viscosity $\nu = 1.5182 \times 10^{-6}\ m^2/s$, and the compressibility $\kappa = 4.217 \times 10^{-10}\ 1/Pa$. The acoustic field is applied to with frequency $\omega = 1.5\ MHz$ with acoustic energy density $E_{ac} = 100\ J/m^3$.

In order to accomplish the effect of ARF, a simple simulation without any bound-

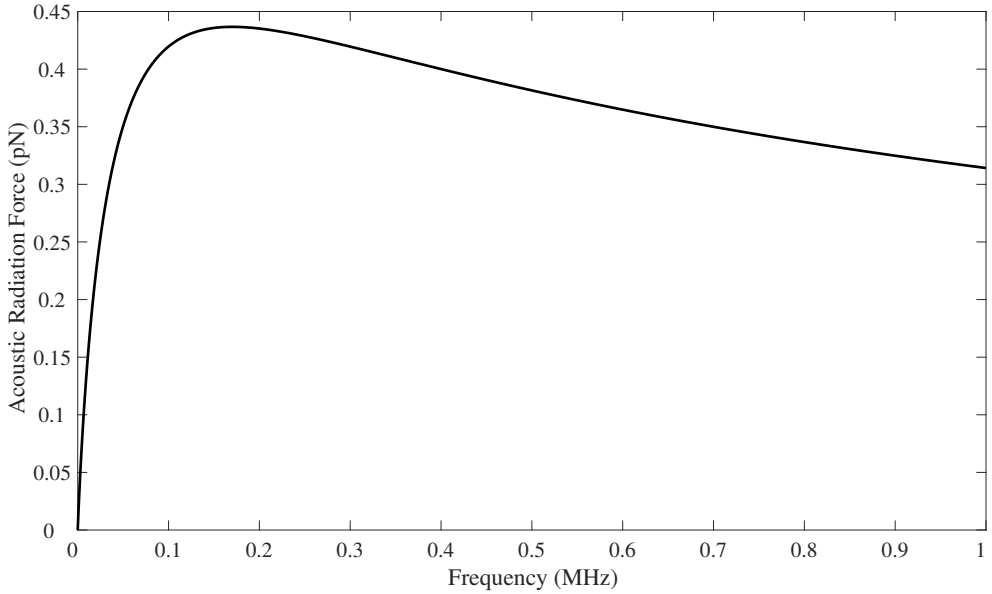

Figure 4.1: ARF vs. Frequency

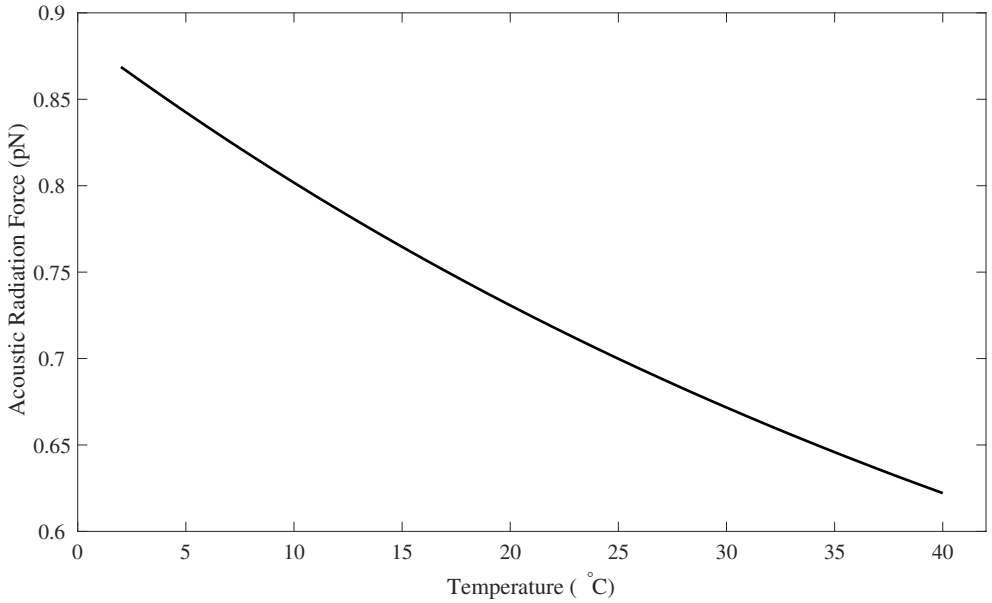

Figure 4.2: ARF vs. Temperature.

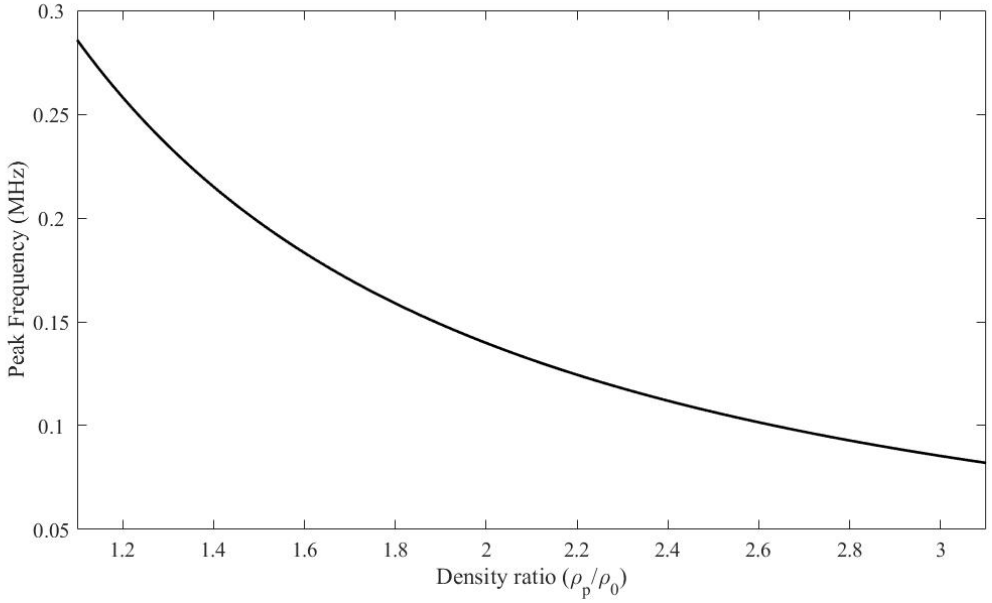

Figure 4.3: Density ratio vs. Frequency

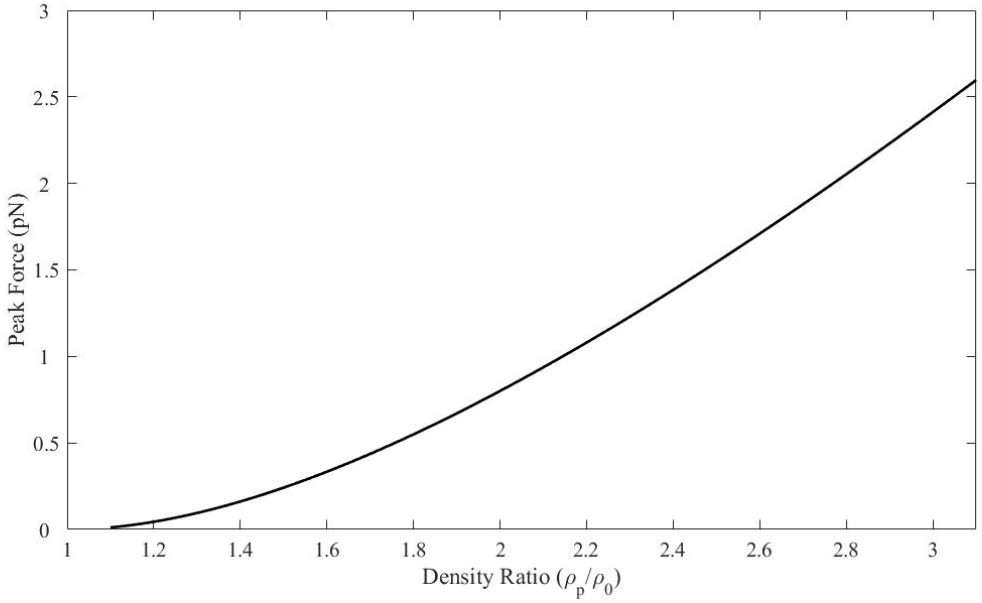

Figure 4.4: Density ratio vs. ARF

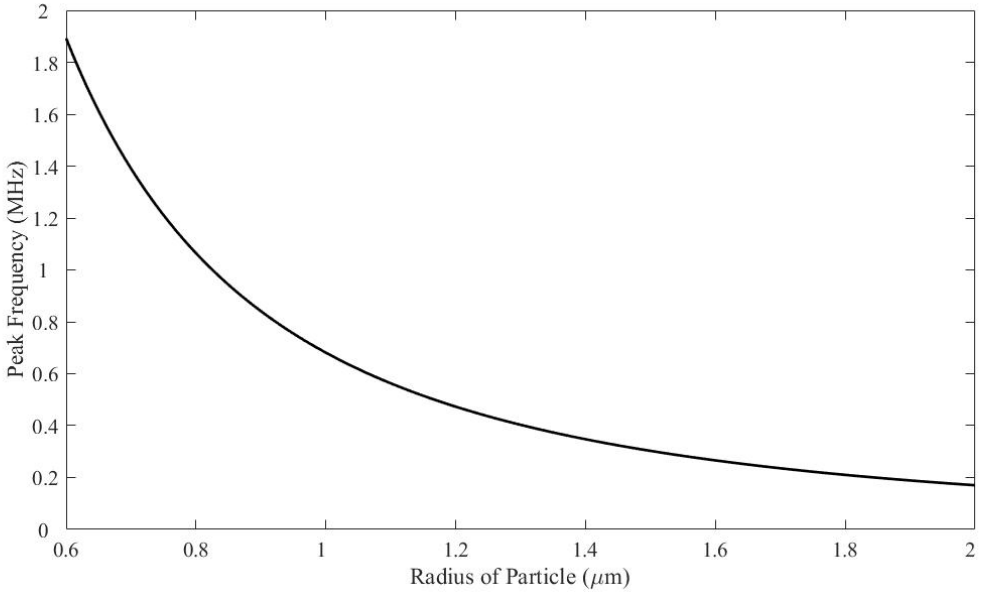

Figure 4.5: Particle radius vs. Frequency

ary conditions and any other external effects was performed. Figures (4.6) for Vicsek model and (4.7) for ABPs show these results. In both simulations, initially 500 particles of radius $r = 2\ \mu m$ were contained in a box of dimensions $150\ \mu m \times 250\ \mu m$, then they are released in vicinity of acoustic fields. It can be clearly seen that the particles in the model of Vicsek almost lost their collective properties since the correlation between them arises with the decreasing distance. Despite this condition, it can be seen that the swarming behavior was still present around the center of mass. On the other hand, apart from the effect of ARF, the motion of ABPs looks completely irregular. The mean squared displacement of a particle is much larger than the ordinary Brownian particle as a consequence of the velocity dependent term. In both cases, the motion of particles is dominated by ARF and the average position of whole community is shifted towards the direction of acoustic waves. Tables (4.2) and (4.1) shows the values of average displacements of particles for different temperatures and frequencies. It can be clearly seen that with increasing temperature, because of the decreasing viscosity, the average displacement increases and the force is much more effective. However, for a higher efficiency, using a low frequency tranducer (though not lower than 100 KHz) would be appropriate.

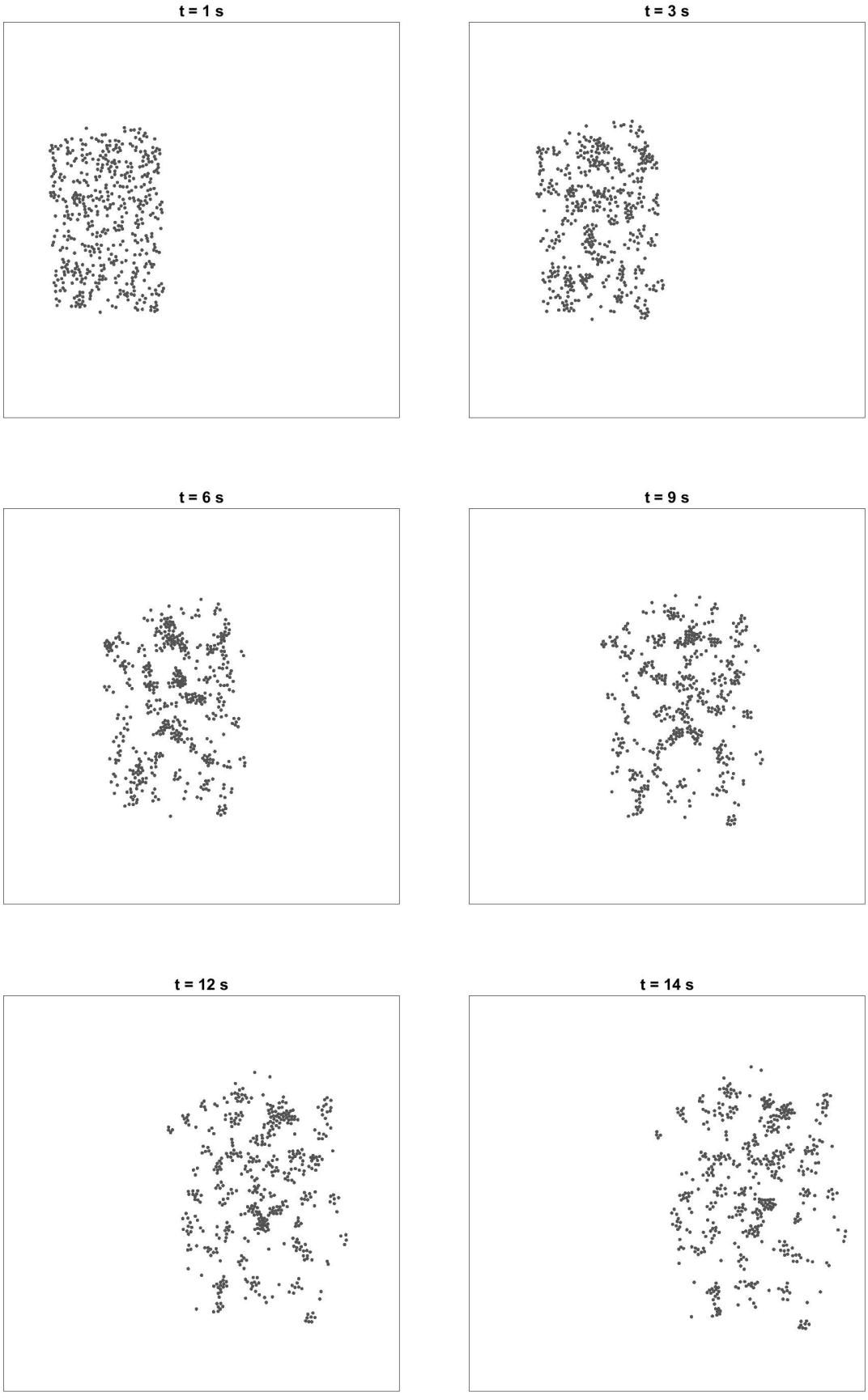

Figure 4.6: Vicsek particles in presence of ARF

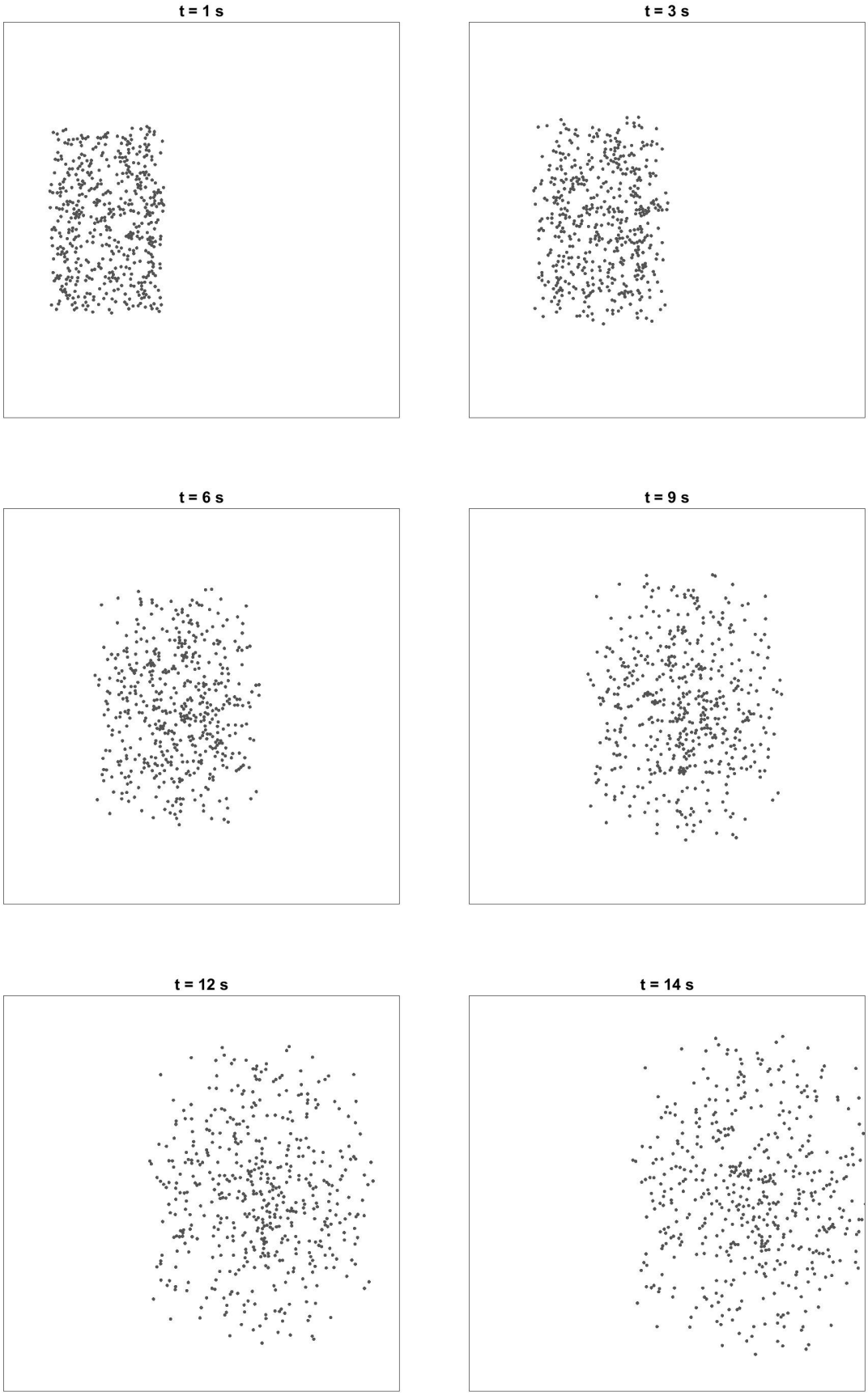

Figure 4.7: ABPs in presence of ARF

Table 4.1: Average displacement of particles in 10 s according to the Vicsek model in the presence of ARF for different temperatures and frequencies.

Temperature (C)	**Frequency (MHz)**	**Average displacement** $\langle \Delta x \rangle$ (μm)
5	0.5	171.0 ± 24.0
	1.0	143.5 ± 22.2
	1.5	128.8 ± 22.4
15	0.5	216.3 ± 24.1
	1.0	174.1 ± 29.5
	1.5	147.0 ± 23.6
25	0.5	260.4 ± 21.2
	1.0	202.3 ± 21.2
	1.5	177.6 ± 21.6

Table 4.2: Average displacement of particles in 10 s according to the ABP model in the presence of ARF for different temperatures and frequencies.

Temperature (C)	**Frequency (MHz)**	**Average displacement** $\langle \Delta x \rangle$ (μm)
5	0.5	177.4 ± 43.8
	1.0	146.9 ± 45.0
	1.5	128.9 ± 44.4
15	0.5	220.2 ± 44.7
	1.0	178.6 ± 43.3
	1.5	154.7 ± 43.3
25	0.5	265.6 ± 45.2
	1.0	209.3 ± 43.3
	1.5	179.7 ± 42.8

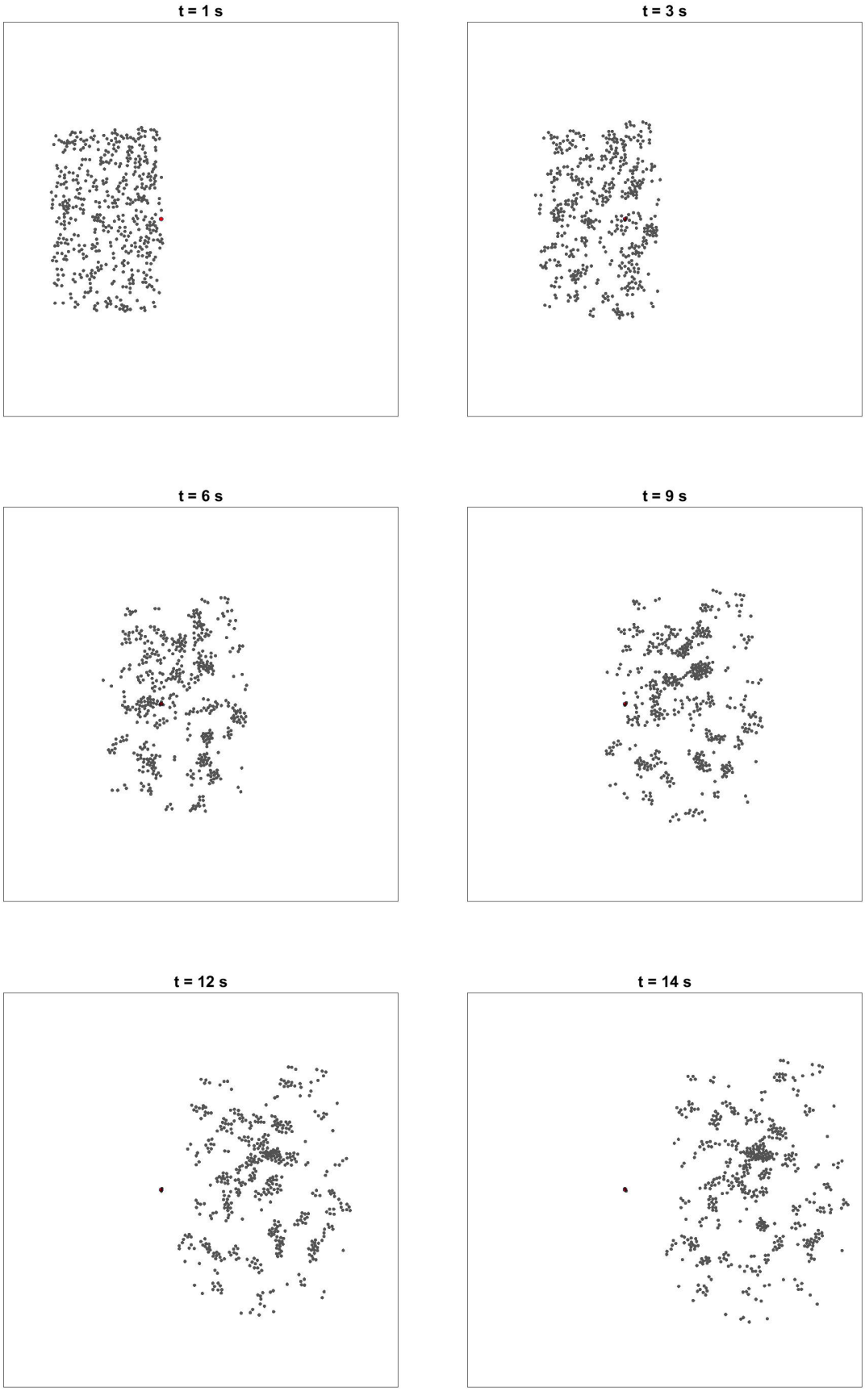

Figure 4.8: Vicsek model in presence of ARF and optical trap

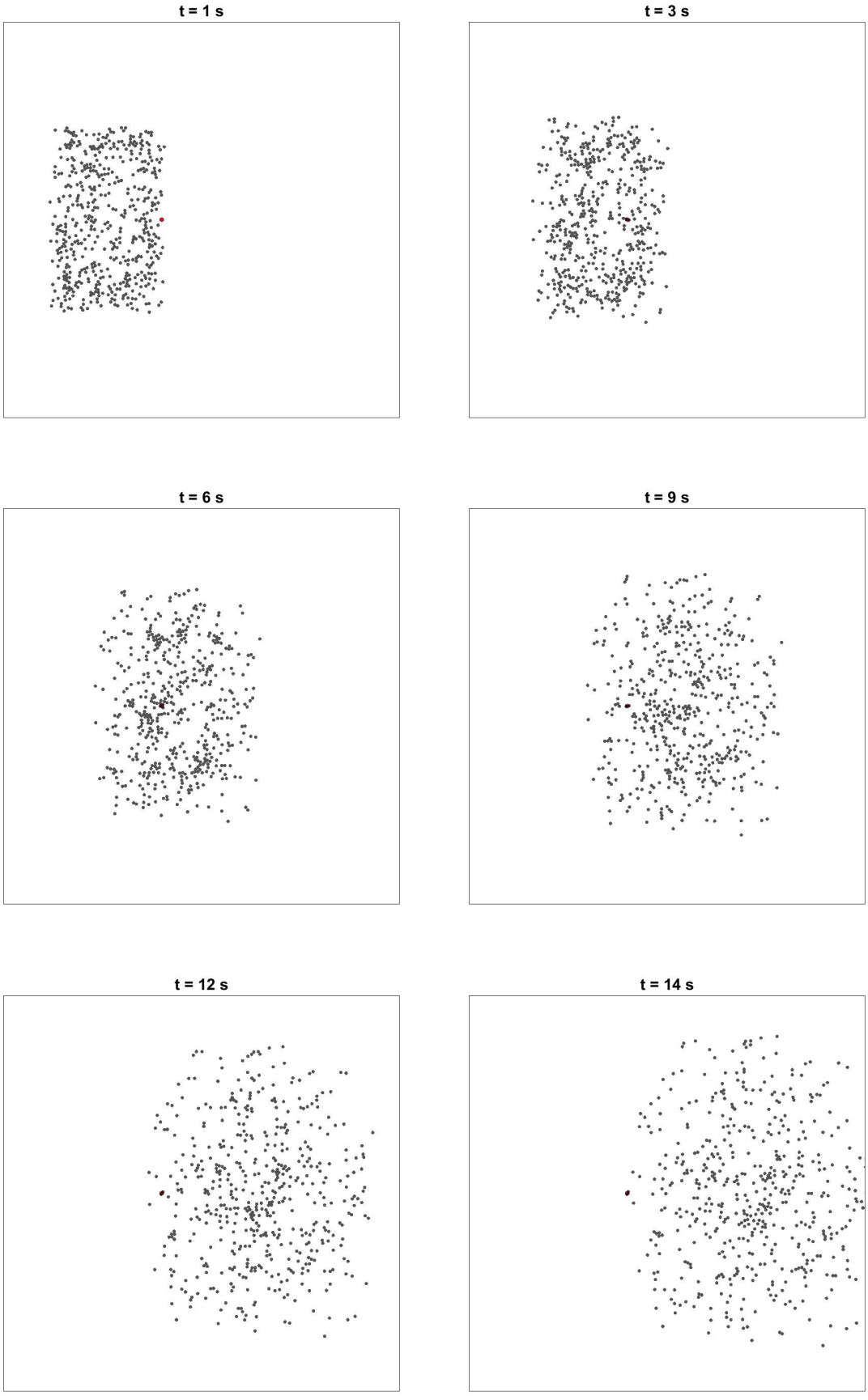

Figure 4.9: ABPs in presence of ARF and optical trap

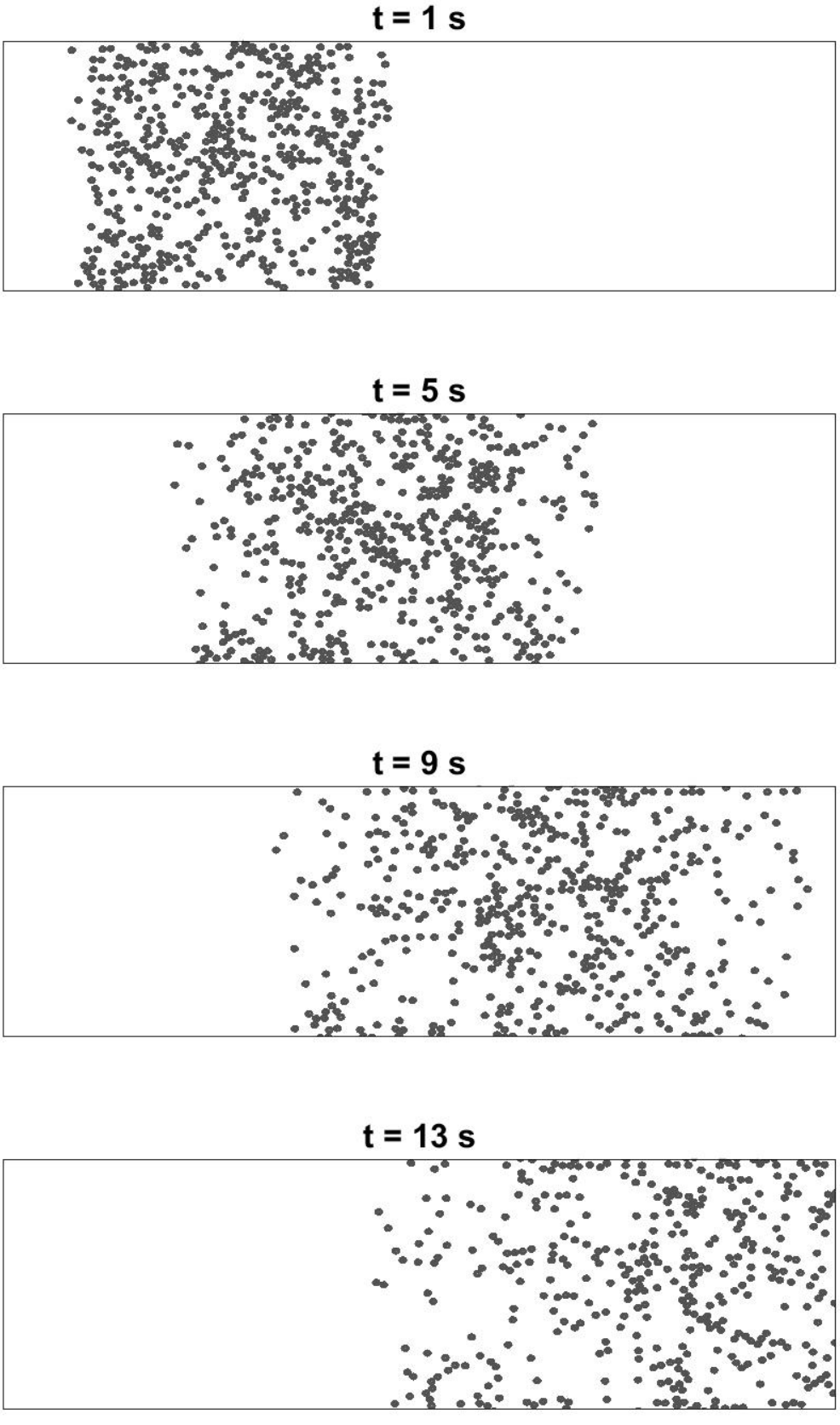

Figure 4.10: ABPs with reflective walls

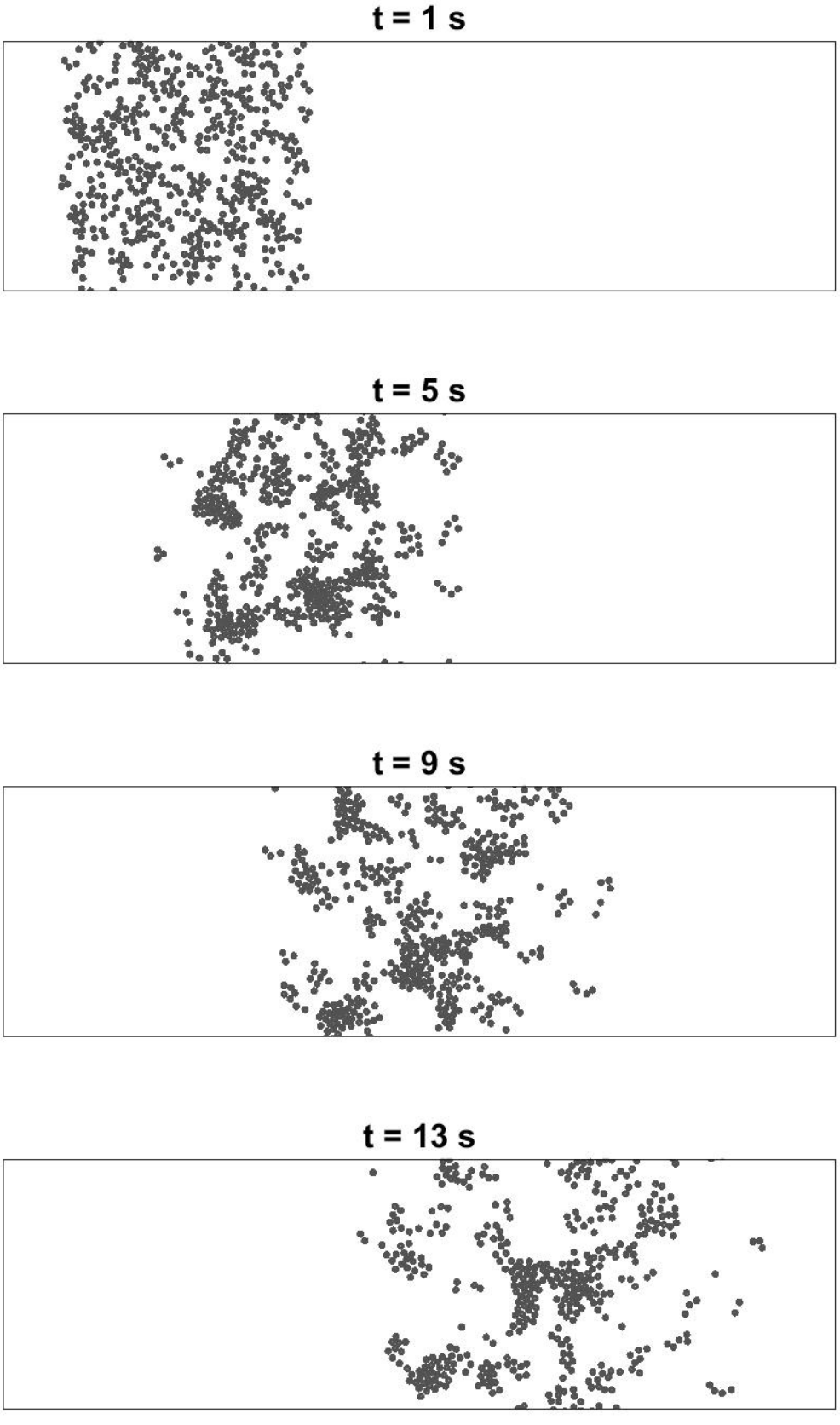

Figure 4.11: Vicsek model with reflective walls

An individual particle can be eliminated selectively by using an optical tweezers. As given in the Section (3.6), in the proximity of an optical trap the restoring force is larger than ARF, which can capture a single particle while others were being swept out. Simulations performed with optical traps are provided in Figures (4.8) and (4.9) in which the trap is represented by the red dot at the center. All the parameters and initial conditions are the same with the preceding simulations and the trap stiffness κ_{trap} in three dimensions was taken as $(1.2 \times 10^{-6}, 0.8 \times 10^{-6}, 1.2 \times 10^{-6})$ N/m. In reality, the value of stiffness depends on the particle type and laser parameters, and can have values in a wide range [83, 84]. The chosen stiffness in this simulation leads a trap force on the order of pN which is enough to capture a particle in an acoustic field without damaging it.

Another simulation with the reflective walls placed at the bottom and the top of the container is provided in Figures (**??**) and (4.10). The simulation with the Vicsek model is resulted that particles are gathering around the walls despite the reflective property. This is a consequence of the process of the angle determination. Nearby the walls, the average direction angle approaches to zero, hence the aggregation is observed. An analogous result was presented by Filly *et al.* (2014) which stated that active particles were assembled near confinement walls [41]. The presence of acoustic field neither assists nor prevents this attitude, however the general effects of ARF on the motion is still remained. In the case of ABPs, because there is no connection between behaviors of particles, the distribution of particles is uniform but the whole community moves under the effect of acoustic field (Can be moved to discussion with corrections).

The behavior of interacting active particles was also investigated with periodic boundary conditions. The simulation with ABPs did not yield any interesting result, therefore only Vicsek particles are considered. Figure (4.12) shows 500 particles inside a box of dimensions 150 $\mu m \times 150$ μm with periodic walls. In the short run, particles create swarms in random places, however, in the long run all the particles and swarms gather and move in the same direction. In their original paper, Vicsek *et al.* defined

the average velocity of particles

$$v_a = \frac{1}{Nv} \sum_{i=1}^{N} v_i \tag{4.1}$$

which can be used as an order parameter for the community [15]. Initially, the directions of the particles distributed randomly, thence the value of v_a is zero. However, as the limit of the time goes to infinity, the average velocity approaches to 1 which means the motion is ordered as depicted in Figure (4.12). Under the periodic boundary conditions, the presence of an acoustic field causes the system to reach order in a small time (4.13). A quick implication could be made that ARF may be used to boost the order in active matter systems.

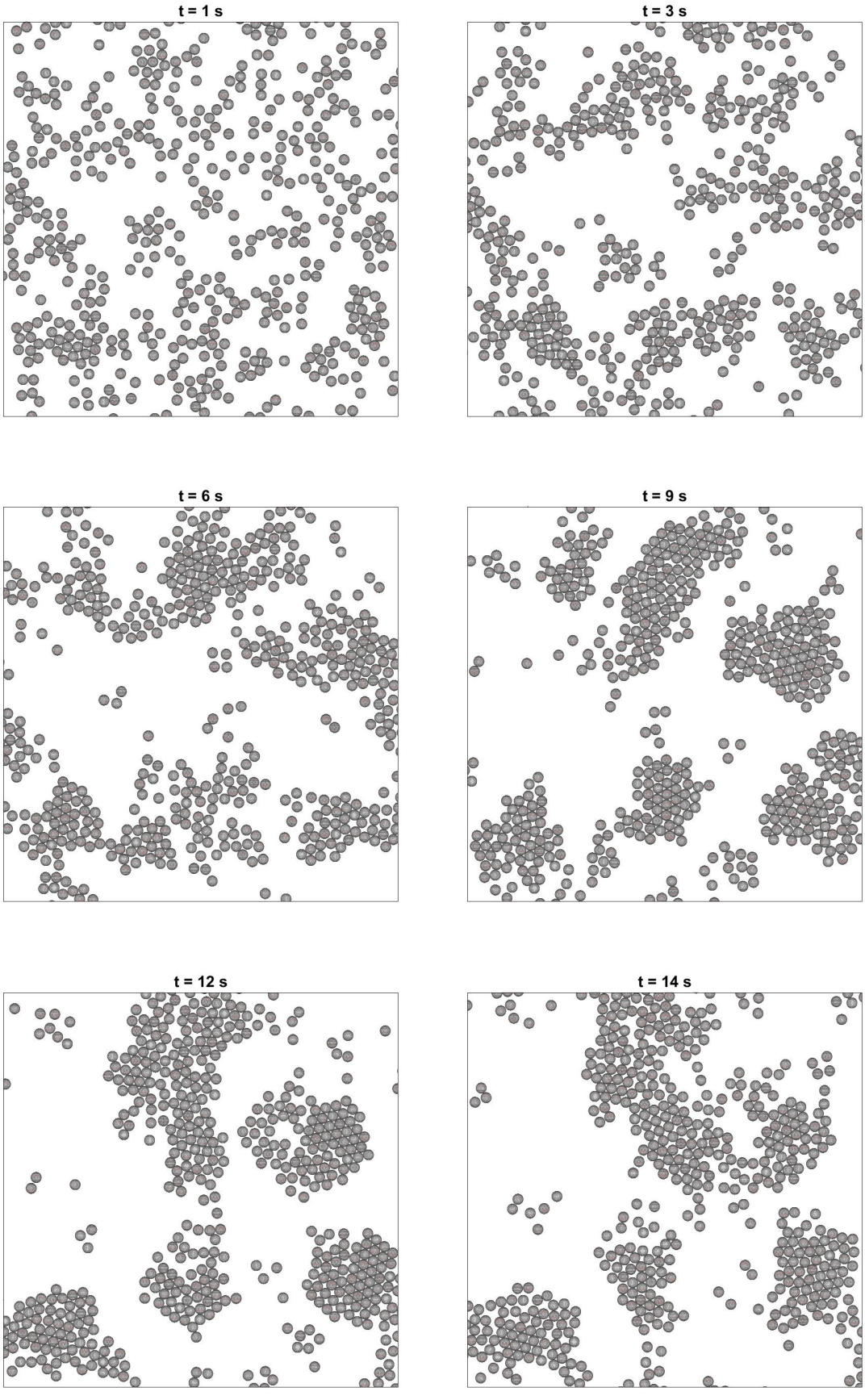

Figure 4.12: Vicsek model with periodic walls

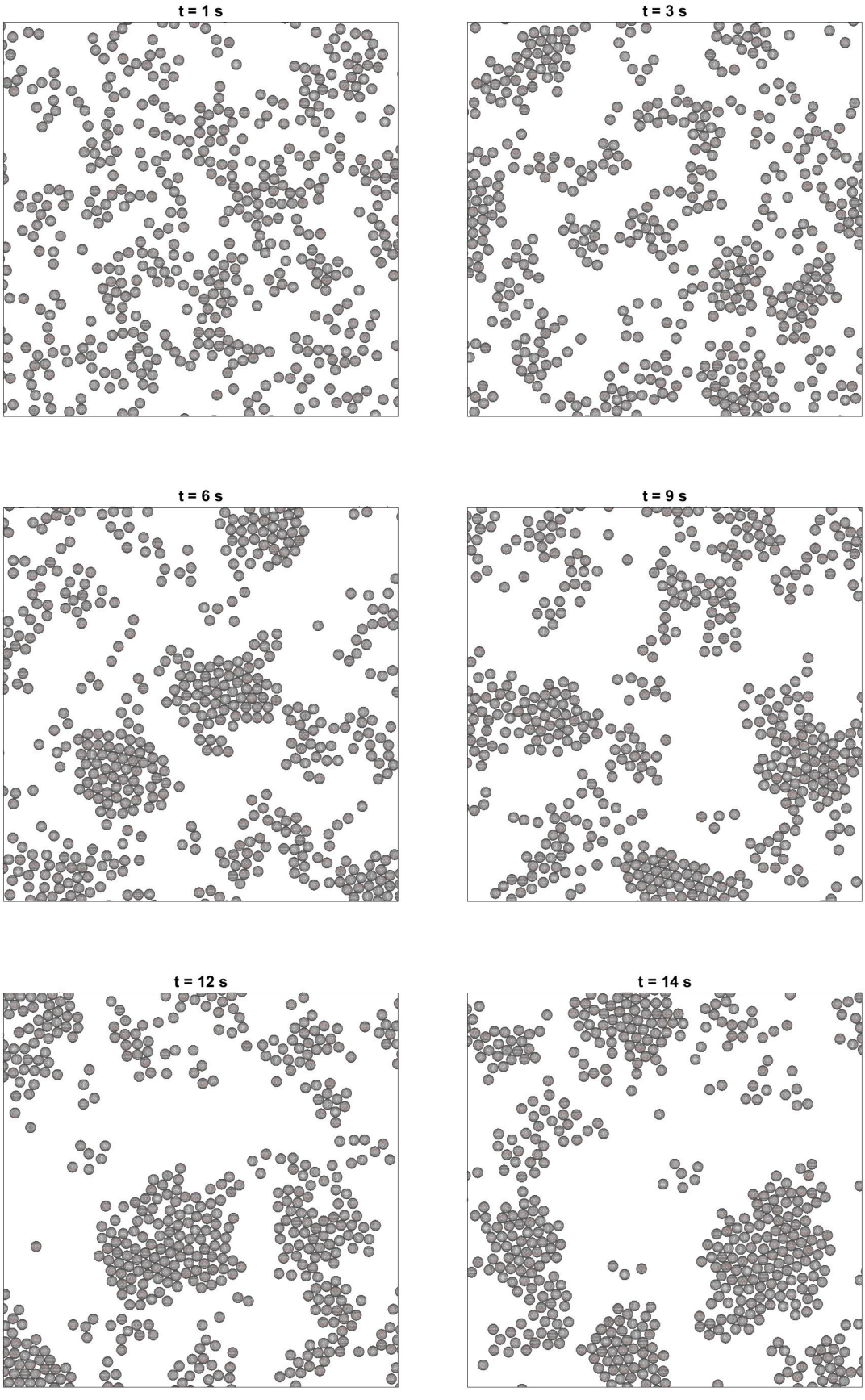

Figure 4.13: Vicsek model with periodic walls in the presence of ARF

5. CONCLUSION

The behavior of self-propelling particles in the presence of an acoustic field has not been studied in detail so far. The lack of research and development makes this topic to preserve its position as an open area. This study proposes the possibility of manipulating active particles in acoustic fields with a so-called *acoustic radiation forces*.

An acoustic wave could be created as standing and/or traveling wave. The application of an acoustic wave into a fluid containing suspended small-sized particles results in ARF experienced by the particles because of the non-uniform pressure distribution. Bruus (2012) stated that for a non-viscous fluid, traveling waves would have no effect on the motion since they created a constant potential across the medium, although it is possible to move particles inside a standing field [82]. However, for a viscous fluid, the motion could be affected by both the standing and traveling waves, even though the force created by traveling waves is much smaller than the force resulted by a standing wave [67]. The basic difference between applied forces of these types of waves is that in a traveling wave field particles can only move in a certain direction while in a standing wave field they would trap in a harmonic potential with long range. In Chapter (1), it is mentioned that some researchers were interested in the motion of active matter inside acoustic fields. Nevertheless, the analytic representation of ARF was not resolved in those studies and there weren't any equations of motion present. Instead of using an acoustic field, those works were concentrated on the behavior of active matter inside a Gaussian harmonic field. In my study, the equation of a motion of an individual particle is dealt with analytically, and solved by numerical methods explained in Chapter (3).

The corresponding frequencies of the peak ARF on active matter is valued in a wide range. Figures (**??**) and (4.5) depicts the relation of corresponding frequencies for different density ratios and radii. An extensive research could be made on the determination of these parameters. The forces on the order of pN can be measured

with spectroscopic methods or optical tweezers, and the ARF on active particles lie in this range. By using these information, the properties of unknown particles could be exploited. Moreover, ARF arises from standing waves could be used in determination and separation of active matter in a crowded environment.

The analysis contained in this document focuses on two different models of active matter. However, as depicted in the Chapter (1), there are numerous models developed for active motion since the particles can have behaviors in variety of individual types. For instance, the so-called run-and-tumble particle model is currently the best explanation for the motion of *Escherichia coli* which is a species of bacteria with flagellum. Nonetheless, the model contains no dynamic equations, instead it describes the motion with probability density functions and hydrodynamic interactions. Thus, the implementation of ARF to the system becomes extremely challenging since those effects are completely ignored in contemplation of simplicity. Energy-depot model, on the other hand, takes energy deposition into account which is a necessary condition for thermodynamic non-equilibrium, and describes the motion of amoeba [16]. In their original study, Schweitzer *et al.* actually used a harmonic potential which could resemble external effects. This potential could be modified with acoustic field parameters, yet the model only explained the behavior of a single particle. The application of that equation into a community yields a complex simulation whereby the relation between particles cannot be resolved. Apart from preceding models, there are also certain descriptions which concentrate on the friction term in Langevin equation. The friction function in these models is usually considered as velocity dependent. Velocity-dependent frictions are not discussed in the document herein because there are numerous types of friction function and they usually contain too many parameters which correspond no physical quantities. Nevertheless, each of the problems explained above should be investigated as a further research topic.

The simulations given in Chapter (4) should be supported experimentally. There were many experimental studies in the literature of active matter, but most of them were model uncorrelated because the required experimental conditions are elusive. However, our approach seems definitely applicable to the experimental conditions, even

though certain problems could be encountered such as the choice of the type of the active particles. t is always possible to extend our study in order to contain all the models, yet further research is required in this manner.

Another implication for this simulations could be the manipulation of particles in lab-on-a-chip devices. By nature, these microfluidic devices contain micron sized channels in which particles can swim. The simulation given in Figures (4.10) and (4.11) could be considered as the motion of particles inside a pipette. Usage of ARF for this purpose can increase the yieldance of the chip.

With active matter models, a wide range of problems could be solved. Apart from the behavior of animal communities or microparticle groups, starting with the Vicsek model, it is possible to model the traffic of a crowded city. Moreover, some growth mechanisms such as tumor growth can be explained by an active matter model in which hydrodynamic interactions are involved. Moreover, controlling human crowds in large areas by changing ambient properties would be possible with these kinds of models.

REFERENCES

1. Dreyfus, R., J. Baudry, M. L. Roper, M. Fermigier, H. A. Stone and J. Bibette, "Microscopic artificial swimmers", *Nature*, Vol. 437, No. 7060, pp. 862–865, 2005.

2. Cavagna, A. and I. Giardina, "Bird flocks as condensed matter", *Annu. Rev. Condens. Matter Phys.*, Vol. 5, No. 1, pp. 183–207, 2014.

3. Mijalkov, M. and G. Volpe, "Sorting of chiral microswimmers", *Soft Matter*, Vol. 9, No. 28, pp. 6376–6381, 2013.

4. Kareiva, P. and N. Shigesada, "Analyzing insect movement as a correlated random walk", *Oecologia*, Vol. 56, No. 2-3, pp. 234–238, 1983.

5. Komin, N., U. Erdmann and L. Schimansky-Geier, "Random walk theory applied to daphnia motion", *Fluctuation and Noise Letters*, Vol. 4, No. 01, pp. L151–L159, 2004.

6. Boedeker, H. U., C. Beta, T. D. Frank and E. Bodenschatz, "Quantitative analysis of random ameboid motion", *EPL (Europhysics Letters)*, Vol. 90, No. 2, p. 28005, 2010.

7. Friedrich, B. M. and F. Jülicher, "Chemotaxis of sperm cells", *Proceedings of the National Academy of Sciences*, Vol. 104, No. 33, pp. 13256–13261, 2007.

8. Selmeczi, D., L. Li, L. I. Pedersen, S. Nrrelykke, P. H. Hagedorn, S. Mosler, N. B. Larsen, E. C. Cox and H. Flyvbjerg, "Cell motility as random motion: a review", *The European Physical Journal Special Topics*, Vol. 157, No. 1, pp. 1–15, 2008.

9. Reimann, P., "Brownian motors: noisy transport far from equilibrium", *Physics reports*, Vol. 361, No. 2, pp. 57–265, 2002.

10. Ebeling, W., F. Schweitzer and B. Tilch, "Active Brownian particles with energy depots modeling animal mobility", *BioSystems*, Vol. 49, No. 1, pp. 17–29, 1999.

11. Howse, J. R., R. A. Jones, A. J. Ryan, T. Gough, R. Vafabakhsh and R. Golestanian, "Self-motile colloidal particles: from directed propulsion to random walk", *Physical review letters*, Vol. 99, No. 4, p. 048102, 2007.

12. Paxton, W. F., K. C. Kistler, C. C. Olmeda, A. Sen, S. K. St. Angelo, Y. Cao, T. E. Mallouk, P. E. Lammert and V. H. Crespi, "Catalytic nanomotors: autonomous movement of striped nanorods", *Journal of the American Chemical Society*, Vol. 126, No. 41, pp. 13424–13431, 2004.

13. Keller, E. F. and L. A. Segel, "Initiation of slime mold aggregation viewed as an instability", *Journal of Theoretical Biology*, Vol. 26, No. 3, pp. 399–415, 1970.

14. Reynolds, C. W., "Flocks, herds and schools: A distributed behavioral model", *ACM SIGGRAPH computer graphics*, Vol. 21, No. 4, pp. 25–34, 1987.

15. Vicsek, T., A. Czirók, E. Ben-Jacob, I. Cohen and O. Shochet, "Novel type of phase transition in a system of self-driven particles", *Physical review letters*, Vol. 75, No. 6, p. 1226, 1995.

16. Schweitzer, F., W. Ebeling and B. Tilch, "Complex motion of Brownian particles with energy depots", *Physical Review Letters*, Vol. 80, No. 23, p. 5044, 1998.

17. Erdmann, U. and W. Ebeling, "Collective motion of Brownian particles with hydrodynamic interactions", *Fluctuation and Noise Letters*, Vol. 3, No. 02, pp. L145–L154, 2003.

18. Guttal, V. and I. D. Couzin, "Social interactions, information use, and the evolution of collective migration", *Proceedings of the national academy of sciences*, Vol. 107, No. 37, pp. 16172–16177, 2010.

19. Pooley, C., G. Alexander and J. Yeomans, "Hydrodynamic interaction between two swimmers at low Reynolds number", *Physical review letters*, Vol. 99, No. 22, p. 228103, 2007.

20. Downton, M. T. and H. Stark, "Simulation of a model microswimmer", *Journal of Physics: Condensed Matter*, Vol. 21, No. 20, p. 204101, 2009.

21. Córdova-Figueroa, U. M. and J. F. Brady, "Osmotic propulsion: the osmotic motor", *Physical review letters*, Vol. 100, No. 15, p. 158303, 2008.

22. Yang, X., M. L. Manning and M. C. Marchetti, "Aggregation and segregation of confined active particles", *Soft matter*, Vol. 10, No. 34, pp. 6477–6484, 2014.

23. Wang, W., W. Duan, Z. Zhang, M. Sun, A. Sen and T. E. Mallouk, "A tale of two forces: simultaneous chemical and acoustic propulsion of bimetallic micromotors", *Chemical Communications*, Vol. 51, No. 6, pp. 1020–1023, 2015.

24. Schimansky-Geier, L., M. Mieth, H. Rosé and H. Malchow, "Structure formation by active Brownian particles", *Physics Letters A*, Vol. 207, No. 3, pp. 140–146, 1995.

25. Soni, G., B. J. Ali, Y. Hatwalne and G. Shivashankar, "Single particle tracking of correlated bacterial dynamics", *Biophysical journal*, Vol. 84, No. 4, pp. 2634–2637, 2003.

26. Berke, A. P., L. Turner, H. C. Berg and E. Lauga, "Hydrodynamic attraction of swimming microorganisms by surfaces", *Physical Review Letters*, Vol. 101, No. 3, p. 038102, 2008.

27. Henkes, S., Y. Fily and M. C. Marchetti, "Active jamming: Self-propelled soft particles at high density", *Physical Review E*, Vol. 84, No. 4, p. 040301, 2011.

28. Volpe, G., I. Buttinoni, D. Vogt, H.-J. Kümmerer and C. Bechinger, "Microswim-

mers in patterned environments", *Soft Matter*, Vol. 7, No. 19, pp. 8810–8815, 2011.

29. Wang, S. and P. G. Wolynes, "On the spontaneous collective motion of active matter", *Proceedings of the National Academy of Sciences*, Vol. 108, No. 37, pp. 15184–15189, 2011.

30. Dey, S., D. Das and R. Rajesh, "Spatial structures and giant number fluctuations in models of active matter", *Physical review letters*, Vol. 108, No. 23, p. 238001, 2012.

31. Peruani, F., J. Starruß, V. Jakovljevic, L. Søgaard-Andersen, A. Deutsch and M. Bär, "Collective motion and nonequilibrium cluster formation in colonies of gliding bacteria", *Physical review letters*, Vol. 108, No. 9, p. 098102, 2012.

32. Stenhammar, J., A. Tiribocchi, R. J. Allen, D. Marenduzzo and M. E. Cates, "Continuum theory of phase separation kinetics for active Brownian particles", *Physical review letters*, Vol. 111, No. 14, p. 145702, 2013.

33. Palacci, J., S. Sacanna, A. P. Steinberg, D. J. Pine and P. M. Chaikin, "Living crystals of light-activated colloidal surfers", *Science*, Vol. 339, No. 6122, pp. 936–940, 2013.

34. Wang, Z., H.-Y. Chen, Y.-J. Sheng and H.-K. Tsao, "Diffusion, sedimentation equilibrium, and harmonic trapping of run-and-tumble nanoswimmers", *Soft Matter*, Vol. 10, No. 18, pp. 3209–3217, 2014.

35. Ray, D., C. Reichhardt and C. O. Reichhardt, "Casimir effect in active matter systems", *Physical Review E*, Vol. 90, No. 1, p. 013019, 2014.

36. Fily, Y., S. Henkes and M. C. Marchetti, "Freezing and phase separation of self-propelled disks", *Soft Matter*, Vol. 10, No. 13, pp. 2132–2140, 2014.

37. Ginot, F., I. Theurkauff, D. Levis, C. Ybert, L. Bocquet, L. Berthier and C. Cottin-

Bizonne, "Nonequilibrium equation of state in suspensions of active colloids", *Physical Review X*, Vol. 5, No. 1, p. 011004, 2015.

38. Loi, D., S. Mossa and L. F. Cugliandolo, "Effective temperature of active matter", *Physical Review E*, Vol. 77, No. 5, p. 051111, 2008.

39. Nash, R., R. Adhikari, J. Tailleur and M. Cates, "Run-and-tumble particles with hydrodynamics: sedimentation, trapping, and upstream swimming", *Physical review letters*, Vol. 104, No. 25, p. 258101, 2010.

40. Mallory, S., A. Šarić, C. Valeriani and A. Cacciuto, "Anomalous thermomechanical properties of a self-propelled colloidal fluid", *Physical Review E*, Vol. 89, No. 5, p. 052303, 2014.

41. Fily, Y., A. Baskaran and M. F. Hagan, "Dynamics of self-propelled particles under strong confinement", *Soft Matter*, Vol. 10, No. 30, pp. 5609–5617, 2014.

42. Solon, A. P., J. Stenhammar, R. Wittkowski, M. Kardar, Y. Kafri, M. E. Cates and J. Tailleur, "Pressure and phase equilibria in interacting active Brownian spheres", *Physical review letters*, Vol. 114, No. 19, p. 198301, 2015.

43. Takatori, S. C. and J. F. Brady, "Swim stress, motion, and deformation of active matter: effect of an external field", *Soft Matter*, Vol. 10, No. 47, pp. 9433–9445, 2014.

44. Couzin, I. D., J. Krause, N. R. Franks and S. A. Levin, "Effective leadership and decision-making in animal groups on the move", *Nature*, Vol. 433, No. 7025, pp. 513–516, 2005.

45. Sumpter, D., J. Buhl, D. Biro and I. Couzin, "Information transfer in moving animal groups", *Theory in biosciences*, Vol. 127, No. 2, pp. 177–186, 2008.

46. Dhar, P., T. M. Fischer, Y. Wang, T. Mallouk, W. Paxton and A. Sen, "Au-

tonomously moving nanorods at a viscous interface", *Nano letters*, Vol. 6, No. 1, pp. 66–72, 2006.

47. Alexander, G. P. and J. M. Yeomans, "Dumb-bell swimmers", *EPL (Europhysics Letters)*, Vol. 83, No. 3, p. 34006, 2008.

48. Di Leonardo, R., L. Angelani, D. Dell'Arciprete, G. Ruocco, V. Iebba, S. Schippa, M. Conte, F. Mecarini, F. De Angelis and E. Di Fabrizio, "Bacterial ratchet motors", *Proceedings of the National Academy of Sciences*, Vol. 107, No. 21, pp. 9541–9545, 2010.

49. Dunkel, J., V. B. Putz, I. M. Zaid and J. M. Yeomans, "Swimmer-tracer scattering at low Reynolds number", *Soft Matter*, Vol. 6, No. 17, pp. 4268–4276, 2010.

50. Putz, V. B. and J. Dunkel, "Low Reynolds number hydrodynamics of asymmetric, oscillating dumbbell pairs", *The European Physical Journal Special Topics*, Vol. 187, No. 1, pp. 135–144, 2010.

51. Sanchez, T., D. T. Chen, S. J. DeCamp, M. Heymann and Z. Dogic, "Spontaneous motion in hierarchically assembled active matter", *Nature*, Vol. 491, No. 7424, pp. 431–434, 2012.

52. Takatori, S. C., W. Yan and J. F. Brady, "Swim pressure: stress generation in active matter", *Physical review letters*, Vol. 113, No. 2, p. 028103, 2014.

53. Leoni, M., J. Kotar, B. Bassetti, P. Cicuta and M. C. Lagomarsino, "A basic swimmer at low Reynolds number", *Soft Matter*, Vol. 5, No. 2, pp. 472–476, 2009.

54. Joanny, J.-F. and S. Ramaswamy, "A drop of active matter", *Journal of Fluid Mechanics*, Vol. 705, pp. 46–57, 2012.

55. Marchetti, M., J. Joanny, S. Ramaswamy, T. Liverpool, J. Prost, M. Rao and R. A. Simha, "Hydrodynamics of soft active matter", *Reviews of Modern Physics*,

Vol. 85, No. 3, p. 1143, 2013.

56. Elgeti, J., R. G. Winkler and G. Gompper, "Physics of microswimmers' single particle motion and collective behavior: a review", *Reports on progress in physics*, Vol. 78, No. 5, p. 056601, 2015.

57. Purcell, E. M., "Life at low Reynolds number", *Am. J. Phys*, Vol. 45, No. 1, pp. 3–11, 1977.

58. Nelson, P. and S. Doniach, "Biological physics: Energy, information life", *Physics Today*, Vol. 57, No. 11, pp. 63–64, 2004.

59. Wiener, C., "Erklärung des atomistischen Wesens des tropfbar-flüssigen Körperzustandes, und Bestätigung desselben durch die sogenannten Molecularbewegungen", *Annalen der Physik*, Vol. 194, No. 1, pp. 79–94, 1863.

60. Gouy, M., "que l'expérience confirme en général.", *J. Phys. Théor. Appliquée*, 1888.

61. Einstein, A., "Un the movement of small particles suspended in statiunary liquids required by the molecular-kinetic theory 0f heat", *Ann. Phys*, Vol. 17, pp. 549–560, 1905.

62. Einstein, A., "Zur theorie der brownschen bewegung", *Annalen der physik*, Vol. 324, No. 2, pp. 371–381, 1906.

63. Von Smoluchowski, M., "Zur kinetischen theorie der brownschen molekularbewegung und der suspensionen", *Annalen der physik*, Vol. 326, No. 14, pp. 756–780, 1906.

64. Langevin, P., "Sur la théorie du mouvement brownien", *CR Acad. Sci. Paris*, Vol. 146, No. 530-533, p. 530, 1908.

65. van Teeffelen, S. and H. Löwen, "Dynamics of a Brownian circle swimmer", *Physical*

Review E, Vol. 78, No. 2, p. 020101, 2008.

66. Romanczuk, P., M. Bär, W. Ebeling, B. Lindner and L. Schimansky-Geier, "Active brownian particles", *The European Physical Journal Special Topics*, Vol. 202, No. 1, pp. 1–162, 2012.

67. Settnes, M. and H. Bruus, "Forces acting on a small particle in an acoustical field in a viscous fluid", *Physical Review E*, Vol. 85, No. 1, p. 016327, 2012.

68. Ashkin, A., "Optical trapping and manipulation of neutral particles using lasers", *Proceedings of the National Academy of Sciences*, Vol. 94, No. 10, pp. 4853–4860, 1997.

69. Rasmussen, M. B., L. B. Oddershede and H. Siegumfeldt, "Optical tweezers cause physiological damage to Escherichia coli and Listeria bacteria", *Applied and environmental microbiology*, Vol. 74, No. 8, pp. 2441–2446, 2008.

70. King, L. V., "On the acoustic radiation pressure on spheres", *Proceedings of the Royal Society of London A: Mathematical, Physical and Engineering Sciences*, Vol. 147, pp. 212–240, The Royal Society, 1934.

71. Yosioka, K. and Y. Kawasima, "Acoustic radiation pressure on a compressible sphere", *Acta Acustica united with Acustica*, Vol. 5, No. 3, pp. 167–173, 1955.

72. Gor'Kov, L., "On the forces acting on a small particle in an acoustical field in an ideal fluid", *Soviet Physics Doklady*, Vol. 6, p. 773, 1962.

73. Takatori, S. C., R. De Dier, J. Vermant and J. F. Brady, "Acoustic trapping of active matter", *Nature communications*, Vol. 7, 2016.

74. Gardiner, C., "Stochastic methods: a handbook for the natural and social sciences 4th ed.(2009)", .

75. Dill, K. and S. Bromberg, *Molecular driving forces: statistical thermodynamics in*

biology, chemistry, physics, and nanoscience, Garland Science, 2010.

76. Favro, L. D., "Theory of the rotational Brownian motion of a free rigid body", *Physical Review*, Vol. 119, No. 1, p. 53, 1960.

77. Egorichev A. V., C. K. V., Kravchun P. N., "Acoustic boundary layer", *Soviet Physics Journal*, Vol. 22, No. 11, pp. 1200—1204, 1979.

78. Vesely, F. J., *Computational Physics*, Springer, 1994.

79. Comenetz, M., *Calculus: the elements*, World Scientific, 2002.

80. Volpe, G. and G. Volpe, "Simulation of a Brownian particle in an optical trap", *American Journal of Physics*, Vol. 81, No. 3, pp. 224–230, 2013.

81. Oksendal, B., *Stochastic differential equations: an introduction with applications*, Springer Science & Business Media, 2013.

82. Bruus, H., "Acoustofluidics 7: The acoustic radiation force on small particles", *Lab on a Chip*, Vol. 12, No. 6, pp. 1014–1021, 2012.

83. Neuman, K. C. and S. M. Block, "Optical trapping", *Review of scientific instruments*, Vol. 75, No. 9, pp. 2787–2809, 2004.

84. Ghislain, L. P., N. A. Switz and W. W. Webb, "Measurement of small forces using an optical trap", *Review of Scientific Instruments*, Vol. 65, No. 9, pp. 2762–2768, 1994.